A morphometric study of the brain ventricles of patients diagnosed with Chronic Hydrocephalus at Groote Schuur Hospital

By: Reagobaka Lichaba (LCHREA001)

A thesis submitted in fulfilment of the requirements for the degree of Master of Science in Medicine, specialising in Applied Anatomy in the Department of Human Biology.

Supervisors: Dr Kentse Mpolokeng, A/Prof Delva Shamley and Dr Sally Rothemeyer

Division of Clinical Anatomy and Biological Anthropology,

Division of Neurosurgery

University of Cape Town

2023

DECLARATION

I, *Reagobaka Lichaba*, hereby declare that the work on which this dissertation/ thesis is based is my original work (except where acknowledgements indicate otherwise) and that neither the whole work nor any part of it has been, is being, or is to be submitted for another degree in this or any other university.

I empower the university to reproduce for the purpose of research either the whole or any portion of the contents in any manner whatsoever.

I have shared the Turn-it-in report with my supervisors.

Signature: Signed by candidate

Date: 14 June 2024

Contents

Acknowledgements

I would like to express my gratitude to my supervisors, Associate Professor Delva Shamley, Dr Kentse Mpolokeng, Dr Sally Rothemeyer, for their invaluable assistance, knowledge, and expertise.

To Professor Sulaiman Moosa for allowing me to access the Groote Schuur Picture Archiving and Communicating System to collect data.

To Dr Julius Rozmiarek, thank you for your assistance in navigating and working with the Groote Schuur Picture Archiving and Communicating System.

To the patients at Groote Schuur Hospital Radiology Department whose scans I was observing, this research would not have been possible without you.

To Miss Mbalentle Madolo, thank you for being my interobserver and taking the many measurements from all those scans.

To Mr Trevor Mafu, thank you for your assistance and guidance on the statistical analysis.

To my family, thank you for your continuous support, prayers, and words of encouragement, you carried me through every step of this degree.

To the University of Cape Town Postgraduate Funding Office for funding me the past two years.

Abbreviations

AHCP – Acute hydrocephalus

CA – Callosal angle

CCH – Communicating chronic hydrocephalus

CHCP – Chronic hydrocephalus

CHP – Chronic hydrocephalus patients

CI – Confidence interval

CNS – Central nervous system

CON - Controls

CP – Control patients

CSF – Cerebrospinal fluid

CT – Computed tomography

EI – Evans index

ETV – Endoscopic triventriculostomy

F – Fisher's exact test

GSH – Groote Schuur Hospital

HCP – Hydrocephalus

ICC – Intraclass correlation coefficient

ICP – Intracranial pressure

iNPH – Idiopathic normal pressure hydrocephalus

IQR – Interquartile range

LIAS – Late-onset idiopathic aqueduct stenosis

LOVA – Long-standing overt ventriculomegaly

mmHg – Millimetre of mercury

MPR – Multiplanar reconstruction

MRI – Magnetic resonance imaging

MU – Mann Whitney U test

NPH – Normal pressure hydrocephalus

OR – Odds ratio

PACS – Picture archiving and communications digital system

POPIA – Protection of personal information act

PWM – Periventricular white matter

PWMC – Periventricular white matter changes

sNPH – Secondary normal pressure hydrocephalus

UCT – University of Cape Town

VP - Ventriculoperitoneal

VPS – Ventriculoperitoneal shunt

List of Figures

List of Tables

Abstract

Hydrocephalus (HCP) is a cerebrospinal fluid condition of the central nervous system, which when it accumulates causes an increase in ventricular enlargement and raised intracranial pressure (ICP). Raised ICP in a fixed volume space is dangerous as it presses onto the brain parenchyma and the surrounding areas and may damage them. Ventricular enlargement is a radiological indicator of HCP and has been one of the features used to diagnose the condition, with the ICP measurement used to confirm the condition. However, measuring ICP is invasive and puts the brain at risk of bleeding and infections, making it necessary to use non-invasive methods of confirming the condition. This study aims to investigate the clinical features observed on the brain scans of patients with hydrocephalus and seeks to describe the unique shape of the frontal horns and use this shape as a non-invasive diagnostic marker.

The study observed the brain magnetic resonance imaging (MRI) and computed tomography (CT) scans of 150 patients who were suspected or known to have HCP from the Radiology Department at Groote Schuur Hospital. These scans were then divided into three groups, namely, the controls, and chronic and acute hydrocephalus groups. The clinical features commonly observed on the brain scans of patients with HCP were evaluated, their measurements taken, and their shapes recorded. These features were the Evans Index, temporal horn width, third ventricle width and shape, callosal angle, frontal horn shape, Sylvian fissure width and periventricular white matter changes. This morphometric data was then analysed to determine their relationship with HCP. Of the clinical features, the frontal

horn shape has not been described in the literature. Therefore, it was described in this study, and its association with the measurement of ICP was assessed.

There was a statistically significant difference in the morphometric data between the control and chronic HCP groups. In contrast, the difference in the data between the chronic and acute HCP groups was not statistically significant. In all three groups, there was a difference in size between the left and right sides, the right side had smaller measurements than the left. There was a significant difference in frontal horn shape between the chronic and acute HCP groups. Additionally, it was evident that there was a relationship between a specific shape of the frontal horn and the measurement of ICP.

The morphometric data of the clinical features were consistent with the literature, except for the Sylvian fissure width. The data in this study showed that the accumulation of CSF occurred mostly on the left side in the clinical features that compared the sides, perhaps suggesting that the condition favoured the left side. The frontal horn shape was different in the chronic and acute HCP groups, it was described as quadrilateral and round, where the quadrilateral shape correlated with the low-moderate ICP, and the round shape correlated with the high ICP reading. Therefore, the frontal horn shape has the potential to be used in the clinical space as a non-invasive imaging marker when differentiating between chronic and acute HCP patients.

Chapter 1: Introduction

1.1 Background

Hydrocephalus (HCP) is a multifactorial, cerebrospinal fluid (CSF) accumulation condition that eventually leads to ventricular expansion, increasing intracranial pressure (ICP) (Kartal and Algin, 2014; Kahle *et al.*, 2016; Filis *et al.,* 2017). Hydrocephalus can either be congenital, associated with genes that control the development and growth of the brain; or acquired, where it may develop typically as a result of pathological processes affecting ventricular flow (Kahle *et al.*, 2016). The expansion of ventricles is alarming as it increases pressure in the intracranial space, which may damage the surrounding brain cells and cause various neurological symptoms, strokes, or even result in death (Kartal and Algin, 2014). Based on its symptoms, HCP is classified as acute or chronic (Leinonen *et al.*, 2018).

Acute hydrocephalus occurs due to the blockage of intraventricular cerebrospinal fluid (Kartal and Algin, 2014). This blockage, by an adhesion or tumour, prevents the absorption of CSF after circulation (Greitz, 2004). When left untreated, it may have damaging effects, as mentioned above, this medical emergency should be attended to promptly unlike chronic hydrocephalus (Kartal and Algin, 2014).

Chronic hydrocephalus is recognised as a type of HCP that is seen in adults who develop a compensatory mechanism that allows the disease to arrest or remain inactive during childhood (Fukuhara and Luciano, 2001; Edwards *et al.*, 2004; Tuniz *et al.*, 2021). Individuals who have chronic hydrocephalus from childhood may only become symptomatic in adulthood (Dewan *et al.*, 2018; Green *et al.*, 2021; Nakajima *et al.*, 2021). The reason for this is, that the CSF accumulation is compensated for by alternative pathways of its absorption (Edwards *et*

al., 2004). With increasing age, this compensatory mechanism begins to deteriorate, and decompensation follows as a result thus causing HCP (Edwards *et al.*, 2004).

There are different types of chronic hydrocephalus such as normal pressure (idiopathic and secondary), congenital, acquired, and compensated congenital hydrocephalus, long-standing overt ventriculomegaly in adults and late idiopathic aqueduct stenosis. These types of HCP have varying causes and competing definitions, which has resulted in limited epidemiological data (Edwards *et al.*, 2004; Dewan *et al.*, 2018).

One of the types of chronic hydrocephalus, idiopathic normal pressure hydrocephalus (iNPH), which has an unknown aetiology, has an incidence that differs annually from 0.5/100 000 to 5.5/100 000 people (Damasceno, 2015; Agarwal *et al.,* 2016; Leinonen *et al.,* 2018). Many studies have indicated that iNPH has a prevalence of 0.5-2.9% in the elderly population (Andersson *et al.*, 2019; Alvi *et al.*, 2020; Farb and Rovira, 2020), while the meta-analysis conducted in 2018 reported a mean prevalence of 0.4% in this group (Dewan *et al.*, 2018). While the general population globally has a lower mean prevalence of 0.18% (Dewan *et al.*, 2018).

Underdeveloped countries are prone to high numbers of congenital HCP, while developed countries see a high number of acquired HCP (Kahle *et al.*, 2016; Dewan *et al.*, 2018). Congenital HCP accounts for 60% of all new paediatric cases in Africa, Latin America and South-East Asia (Dewan *et al.*, 2018).

However, Africa is lacking in the literature concerning HCP, more specifically that which affects adults (Bir *et al.*, 2016; Dewan *et al.*, 2018). The most well-documented cases to date of HCP are from Uganda, where there is a 60% incidence of post-infectious HCP (Warf, 2005). It is also estimated that childhood HCP will increase by 180 000 new cases annually in Africa,

and many of those individuals will carry the disease to adulthood, necessitating early diagnosis to attempt to reduce that number (Kahle *et al.*, 2016; Dewan *et al.*, 2018).

Diagnosis of HCP relies on symptoms that are noted during patient examination (Kockum *et al.*, 2018); using imaging. Magnetic resonance imaging (MRI) and computed tomography (CT) scans are used to assess the brain and rule out clinical features (Kitagaki *et al.*, 1998; Roblot *et al.*, 2021), as well as measuring the ICP and monitoring it (Evensen and Eide, 2020; Panigrahi *et al.*, 2021). Measuring ICP is an invasive procedure that puts the brain at risk of infection or haemorrhage (Evensen and Eide, 2020; Panigrahi *et al.*, 2021). Therefore, having a non-invasive diagnostic approach could reduce the number of patients who would otherwise have to undergo the invasive procedure of measuring ICP.

1.1.1. Gap in the literature

Research surrounding the diagnosis of chronic HCP has been done in a few countries, namely, Sweden, Japan and the United States of America where they have examined the size of the ventricles and the effects that ventricular enlargement has on surrounding parts of the brain (Dewan *et al.*, 2018; Andersson *et al.*, 2019; Capone *et al.,* 2020; Nakajima *et al.*, 2021). While ventricular morphology and specific parts of the system have played a significant role in the non-invasive detection and diagnosis of chronic HCP (Kockum *et al.*, 2018; Nakajima *et al.*, 2021), the morphology of the frontal horns has not been described in the literature.

1.1.2. Study relevance

Chronic HCP is frequently misdiagnosed due to the similarities observed in the enlargement of ventricular size and alterations in ventricular structure across various conditions like brain atrophy, stroke, Alzheimer's and Parkinson's disease (Xu *et al.*, 2022). Therefore, there is a need to identify ways in which the disease can be detected early and accurately so that treatment may follow promptly if required. This is more important because cognitive impairment such as dementia, being one of the symptoms of chronic HCP, is the only type that can be cured, which would improve the lives of those affected by the disease (Andersson *et al.,* 2017; Capone *et al.*, 2020).

In addition to detecting the disease with increased accuracy and timeously, this study seeks to describe an imaging marker that will potentially serve as an alternative, non-invasive method of measuring ICP to diagnose chronic HCP.

1.1.3. Purpose of study

The purpose of the study is to examine the frontal horn shape of chronic and acute HCP patients and to explore its potential utility as an imaging diagnostic marker to increase diagnostic accuracy.

The hypothesis is that the frontal horn morphology will serve as a unique, unstudied clinical feature of the lateral ventricles of patients with chronic HCP.

1.1.4. Study aim

To describe whether ventricular morphometrics can be used to differentiate between acute and chronic hydrocephalus.

1.1.5. Study objectives

2. To measure and record the size of the ventricles and other CSF spaces.
3. To describe the morphology of the frontal horns which pertains to the shape of the ventricles.
4. To explore the association between the morphometric data and the diagnosis of hydrocephalus.

The current study's findings are intended to potentially serve as a non-invasive diagnostic marker when a patient is examined. If this imaging biomarker can be shown to be accurate in differentiating acute (requiring CSF diversion) from chronic or arrested (not requiring CSF diversion) hydrocephalus, many patients could be saved from unnecessary procedures.

Chapter 2: Literature Review

2.1 The anatomy of the ventricular system

The ventricular system of the brain consists of four cavities known as ventricles, namely, the paired lateral ventricles, and the third and fourth ventricles, as shown in Figure 2.1 (Stratchko *et al.*, 2016). Each ventricle has its choroid plexus which is made up of a network of ependymal cells that produce CSF (Mortazavi *et al.,* 2014). This fluid circulates within the ventricular system, subarachnoid spaces and the central canal (Filis *et al.,* 2017).

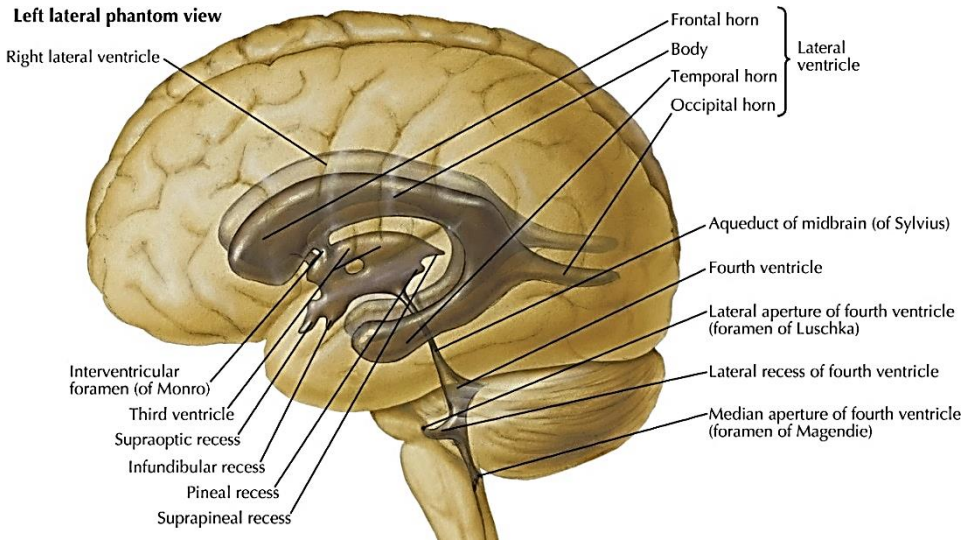

Figure 2.1: Ventricles of the brain (Netter, 2023). Copyright 2022 by Elsevier.

2.1.1 The lateral ventricles

The lateral ventricles consist of anterior, posterior, and inferior horns that form a C-shaped structure that is composed of a body and an atrium (Stratchko *et al.*, 2016). The horns project into the frontal, occipital and temporal lobes, respectively. Superior to the lateral ventricles,

is the corpus callosum and inferiorly is the paired thalami (Scelsi *et al.*, 2020). The atrium is a trigone structure, communicating with the bodies of the lateral ventricles, occipital (posterior) and temporal (inferior) horns, as seen in Figure 2.2 (Mortazavi *et al.*, 2014). How the lateral ventricles communicate with the third ventricle is through the interventricular foramen (of Monro) (Scelsi *et al.*, 2020).

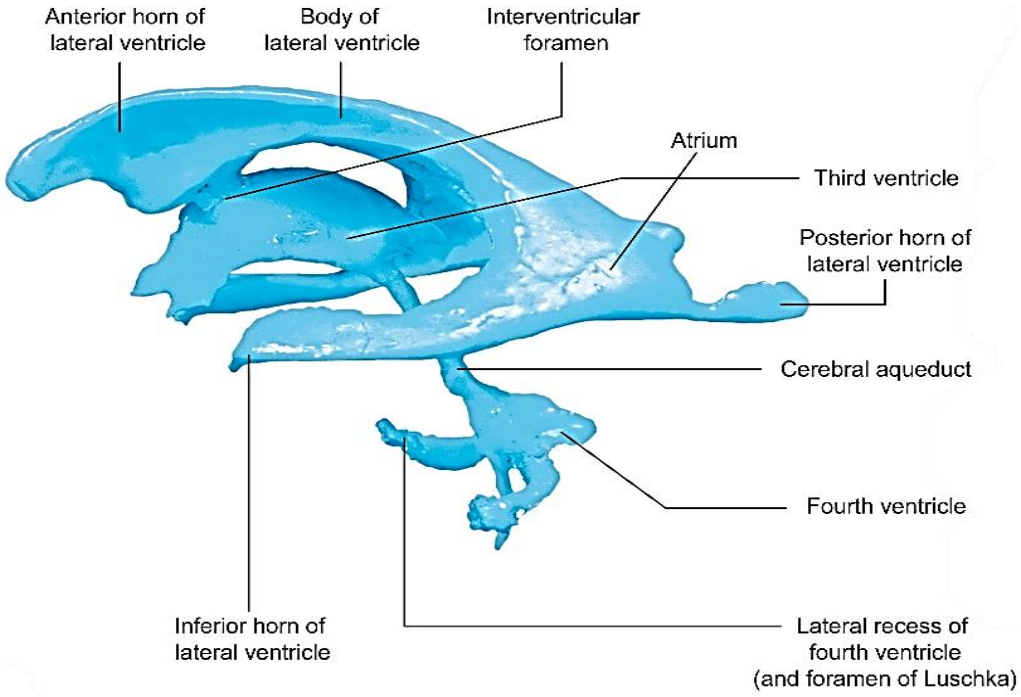

Figure 2.2: Components of the ventricular system represented by a resin cast (Crossman, 2020). Copyright 2024 by Elsevier.

2.1.2 The third ventricle

The third ventricle has the shape of a funnel and is quite narrow, lying between the left and the right sides of the diencephalon. It communicates with the lateral ventricles above via the

interventricular foramen and with the fourth ventricle below, via the cerebral aqueduct (Mortazavi *et al.*, 2014).

2.1.3 The fourth ventricle

It is diamond-like in shape and is located between the brainstem anteriorly and the cerebellum posteriorly. Its floor is formed by the dorsal part of the pons and the upper part of the medulla oblongata (Biga *et al.,* 2019). It is connected superiorly to the third ventricle via the cerebral aqueduct, which passes through the midbrain, and it is connected inferiorly with the central canal (Adigun and Al-Dhahir, 2021).

2.2 Cerebrospinal fluid

Cerebrospinal fluid secretion is vital as it ensures that the environment surrounding the brain and spinal cord is always kept stable (Telano & Baker, 2021). CSF aids in protecting the brain, absorbing mechanical forces, supplying the brain with nutrients, as well as removing waste from it (Stratchko *et al.,* 2016). Additionally, it keeps the brain buoyant and protects it from neurotoxins (Tumani *et al.,* 2018). It is also known to aid in detecting disorders of the central nervous system (CNS) (Tumani *et al.,* 2018), which is achieved via a lumbar puncture or by withdrawing the CSF from the cerebral cisterns, although, the latter is not a preferred method as it is invasive (Sakka *et al.,* 2011).

2.2.1 Cerebrospinal fluid hydrodynamics

The physiological volume of CSF ranges from 90-200ml in adults, and has a turnover of 500ml (Leinonen *et al.,* 2018), with the majority of the volume in the subarachnoid spaces in the intracranial space, the spine, and the rest in the ventricles. The normal CSF pressure in a supine position is 8-15mmHg and 20mmHg in an erect position and this pressure is controlled during CSF secretion and absorption (Adigun & Al-Dhahir, 2021). An increase in these values could be indicative of intracranial hypertension. Additionally, the volume of CSF present in the spaces it occupies determines the size of these spaces, i.e. the ventricles which change size to accommodate the changes in CSF volume (Telano & Baker, 2021).

About 80% of the CSF is secreted by the choroid plexus, the remaining 20% is secreted by the ependymal cells and the brain parenchyma (Brinker *et al.,* 2014). The CSF is produced in two stages: stage one occurs across permeable endothelial capillaries, where passive filtration is allowed, whereas stage two involves the fluid actively passing into the ventricular space across the choroidal epithelium (Khasawneh *et al.,* 2018). The rate of CSF secretion is 0.3 – 0.4mL/min and needs to remain within this range to maintain a balance between secretion and absorption and ensure equilibrium (Tumani *et al.,* 2018).

Equilibrium is also affected by absorption, which is pressure-dependent. Therefore, it is necessary that the pressure gradient that exists between the subarachnoid spaces and that in the venous sinuses ranges from 3 - 5mmHg to make certain that CSF is absorbed (Sakka *et al.,* 2011). The process of absorption occurs via the arachnoid granulations from the subarachnoid space, into the dural venous sinuses to be drained into the circulatory system (Brinker *et al.,* 2014).

2.2.2 The flow of cerebrospinal fluid

The flow of the CSF under normal circumstances follows the following path as shown in Figure 2.3. It traverses the ventricular system by passing through the paired lateral ventricles, then through the interventricular foramen (of Monro), entering the third ventricle, and subsequently flowing into the fourth ventricle through the cerebral aqueduct (of Sylvius). Once in the fourth ventricle, the fluid is drained into the subarachnoid space through the foramen of Magendie and the paired foramina of Luschka for reabsorption (Mortazavi *et al.*, 2014).

A disruption to the flow may cause several disorders such as arachnoid cysts, intracranial hypotension and fistulas between the subarachnoid space and inner ear (Kartal and Algin, 2014), as well as hydrocephalus, which will be the subject of this study.

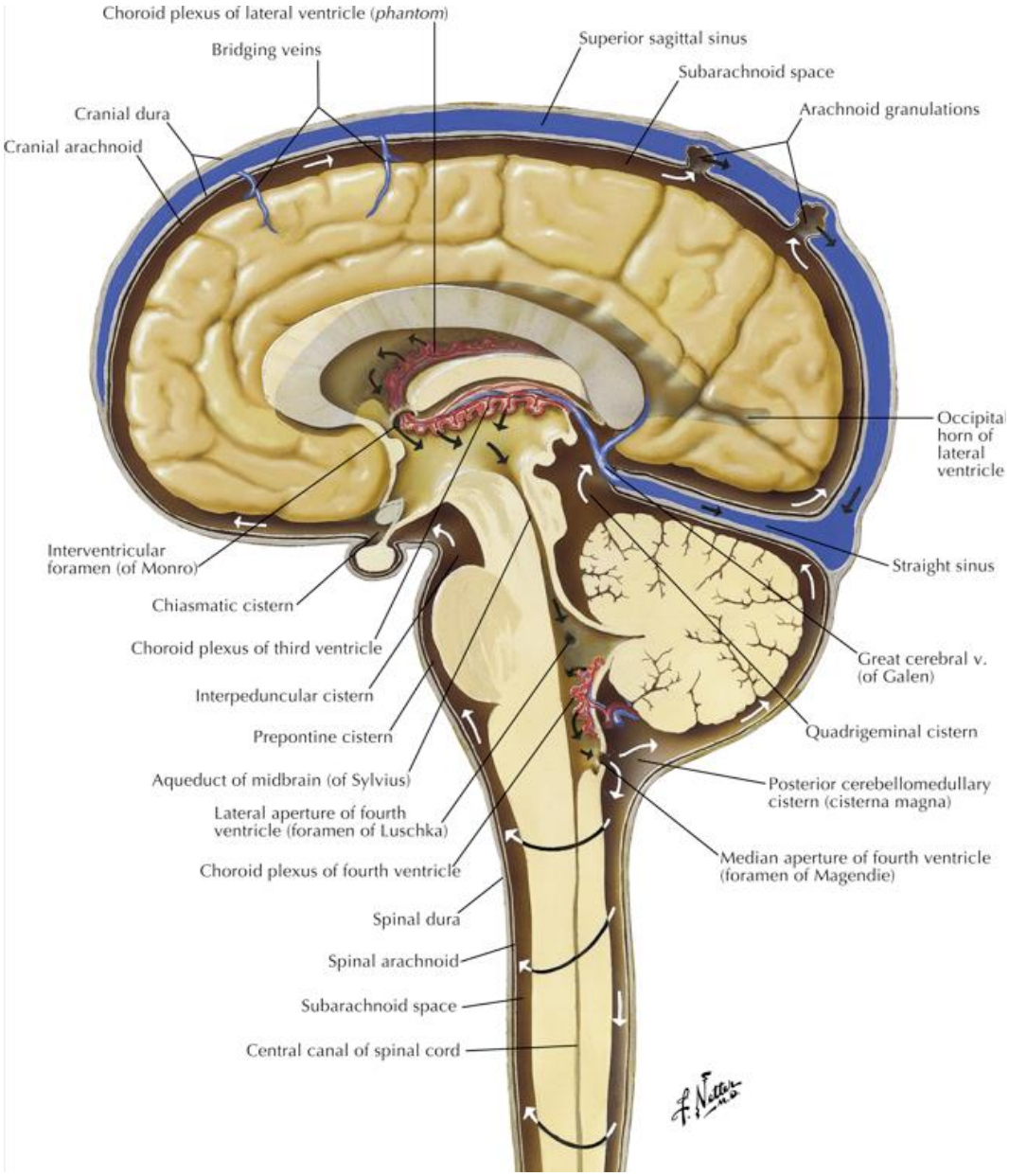

Figure 2.3: An illustration of the circulation of cerebrospinal fluid within the subarachnoid space (Netter, 2023). Copyright 2022 by Elsevier.

2.3 Hydrocephalus

Hydrocephalus is a condition caused by CSF accumulation in the ventricular system due to the disruption of fluid drainage. This accumulation causes an enlargement of the ventricles (Kartal and Algin, 2014). This disorder is classified into two main categories namely: based on its symptoms (Leinonen *et al.,* 2018). Acute hydrocephalus develops when the CSF flow inside the ventricular system is blocked, and chronic hydrocephalus develops when the compensatory mechanism that allowed the disorder to be arrested has failed. Additionally, it is further categorised as either communicating or non-communicating (obstructive), depending on the underlying cause (Kahle *et al.,* 2016).

2.3.1 Communicating chronic hydrocephalus

Communicating chronic hydrocephalus (CCH) affects the entire ventricular system and it arises due to an obstruction outside of the ventricular system (Kitagaki *et al.*, 1998; Leinonen *et al.,* 2018; Yin *et al.,* 2021). Some researchers believe that CCH should further be described as either communicating with or without obstruction because certain types of hydrocephalus do not have an obstruction to CSF flow and absorption (Agarwal *et al.,* 2016; Farb and Rovira, 2020). The pathologies that could obstruct CSF flow include meningitis (bacterial and aseptic), intracerebral haemorrhage and sinus thrombosis (Agarwal *et al.,* 2016; Filis *et al.,* 2017; Farb and Rovira, 2020).

The different types of communicating chronic hydrocephalus include normal pressure hydrocephalus, compensated (arrested) congenital hydrocephalus and congenital

hydrocephalus and these types will each be described briefly (Kitagaki *et al.*, 1998; Leinonen *et al.,* 2018; Yin *et al.,* 2021).

2.3.1.1 Normal pressure hydrocephalus

Normal pressure hydrocephalus (NPH) has no macroscopical obstruction of CSF flow in the entire ventricular system (Edwards *et al.*, 2004; Kartal and Algin, 2014; Leinonen *et al.,* 2018; Roblot *et al.*, 2021). Its appearance has been described as the disproportionate enlargement of the ventricles to the cortical sulci, as well as the expansion of the frontal and temporal horns and surrounding CSF spaces (Edwards *et al.*, 2004; Jaraj *et al.*, 2017; Farb and Rovira, 2020).

Normal pressure hydrocephalus is suspected when there is ventricular enlargement without the clinical symptoms and factors associated with increased intracranial pressure (ICP), note that ICP remains within the normal range (< 20 mmHg) (Edwards *et al.*, 2004; Damasceno, 2015; Filis *et al.,* 2017). Normal pressure hydrocephalus is further divided into two groups, namely: secondary NPH (sNPH), with known causes and idiopathic NPH (iNPH), with unknown causes (Edwards *et al.*, 2004; Agarwal *et al.,* 2016; Yin *et al.,* 2021). Both types are most evident in adults who are over the age of 70 years (Damasceno, 2015; Leinonen *et al.,* 2018; Farb and Rovira, 2020).

2.3.1.1a) Pathophysiology of iNPH

A contribution to the cause of iNPH is the accumulation of CSF in the brain because of an abnormality in its absorption, even when the rate of secretion is constant (Roblot *et al.*, 2021). However, there is an intricate disruption of CSF dynamics that is not fully described (Green *et al.*, 2021).

As the pathophysiology of iNPH is still not fully understood, there have been contributions from hypotheses of neurodegenerative diseases, especially Alzheimer's and Parkinson's disease, as they share clinical features (Andersson *et al.*, 2019; Capone *et al.,* 2020; Roblot *et al.*, 2021; Yin *et al.,* 2021). Even so, the imaging features of iNPH differ from those of neurodegenerative diseases and these will be discussed in greater detail in section 2.4.1 (Andersson *et al.*, 2019). Determining pathophysiology may be assisted by evaluating the morphological features of iNPH (Capone *et al.,* 2020). These features, when studied radiologically, have been proven to correlate with the clinical symptoms of iNPH (Virhammar *et al.*, 2014).

2.3.1.1b) Clinical presentation of iNPH

Clinical presentation depends on the age of a person; whether intracranial hypertension is present (usually in younger adults) or not, as well as co-existing cerebrovascular diseases which are usually present in older adults (Edwards *et al.*, 2004; He *et al.*, 2020). Younger patients may suffer from low-grade non-specific headaches due to moderate intracranial pressure. However, these headaches do not develop with the symptoms such as vomiting and

nausea, related to increased intracranial pressure, only when the headache worsens do patients experience nausea (Edwards *et al.*, 2004; Leinonen *et al.,* 2018). Furthermore, these patients may be susceptible to gradual deterioration of visual acuity as a consequence of chronic papilledema and optic atrophy (Edwards *et al.,* 2003; Edwards *et al.*, 2004).

Older patients will present with the triad of gait imbalance, urinary incontinence and cognitive impairment, as explained by Adams and Hakim in 1965 (Hakim and Adams, 1965). Only 50 - 70% of hydrocephalus cases present with all three symptoms; cognitive impairment and gait imbalance are associated most of the time, while urinary incontinence is not seen often (Roblot *et al.*, 2021).

2.3.1.1c) Diagnosis

As a result of having similar clinical manifestations as other neurodegenerative diseases such as Alzheimer's and Parkinson's disease, iNPH diagnosis now necessitates the exclusion of those diseases (Andersson *et al.*, 2017). This has in turn made diagnosing iNPH challenging (Andersson *et al.*, 2017; Yin *et al.,* 2021), which is the reason iNPH remains underdiagnosed and under-treated (Andersson *et al.*, 2019; Yin *et al.,* 2021). Nonetheless, the exclusion of neurodegenerative diseases is important before any decisions on diagnosis can be made (Roblot *et al.*, 2021; Yin *et al.,* 2021).

2.3.1.2 Compensated congenital hydrocephalus

Compensated congenital hydrocephalus, also known as arrested congenital hydrocephalus, is another type of chronic hydrocephalus. Where a disequilibrium in CSF production and absorption is the common cause, with increased ICP (mean ≤ 12 mmHg) being a consequence of the disorder (Adigun and Al-Dhahir, 2021). In about 50% of the cases, this may resolve by itself if it is not treated, resulting in a return to equilibrium and a decrease in ICP (Panigrahi *et al.*, 2021).

The compensatory mechanism involved in compensated congenital hydrocephalus has many theories have been proposed to try and explain the mechanism, the hypothesis by Oi and Di Rocco (2006), as well as Shen *et al.,* (2006), is that there is a new pathway that is developed to help with absorption (Tuniz *et al.*, 2021). This pathway is the transependymal intraparenchymal pathway, and it allows CSF to pass across the ventricular walls, through the blood-brain barrier, and enter the cerebral capillaries (Tuniz *et al.*, 2021).

2.3.1.2a) Clinical presentation

Patients will present with macrocephaly or neurologic disorders that are either mild or not present at all (Hong *et al.*, 2016; Tuniz *et al.*, 2021). Other symptoms that are related to raised ICP include papilloedema, headaches, nausea, vomiting, and a change in consciousness (Panigrahi *et al.*, 2021). Neurological signs such as ataxia, tremor, dystonia, and a delay in gross motor abilities may arise once compensated congenital hydrocephalus starts to progress (Hong *et al.*, 2016; Panigrahi *et al.*, 2021).

2.3.1.2b) Diagnosis

Magnetic resonance imaging is the most well-known method used to diagnose hydrocephalus (Kitagaki *et al.*, 1998; Roblot *et al.*, 2021). It allows for detailed visualisation of the brain structures including the size and shape of cerebral ventricles and the subarachnoid spaces. By examining these features, an assessment can be concluded whether there is an indication of raised ICP (Panigrahi *et al.*, 2021). The following clinical features are observed in patients who have compensated congenital hydrocephalus: thinning of the walls of the corpus callosum and the wall of the third ventricle changing from a concave shape to a convex or more straight shape (Panigrahi *et al.*, 2021).

2.3.1.3 Congenital hydrocephalus

This type of hydrocephalus occurs in children when the skull has not been completely fused (McAllister, 2012). Congenital hydrocephalus is characterised by skull and ventricular enlargement, increasing ICP, and stretching and compression of the brain tissue (McAllister, 2012; Kahle *et al.*, 2016). The severity of the disorder depends on the age of onset, as well as the extent and period of ventriculomegaly (McAllister, 2012).

Congenital hydrocephalus can be caused by both genetic and acquired factors which are classified into different groups (Figure 2.4) (McAllister, 2012; Dewan *et al.*, 2018; Varela *et al.,* 2020). In most cases, congenital hydrocephalus is related to neurological damage, however, more research is needed to explain the pathogenesis, biological processes and the mechanisms that contribute to this damage (Varela *et al.,* 2020).

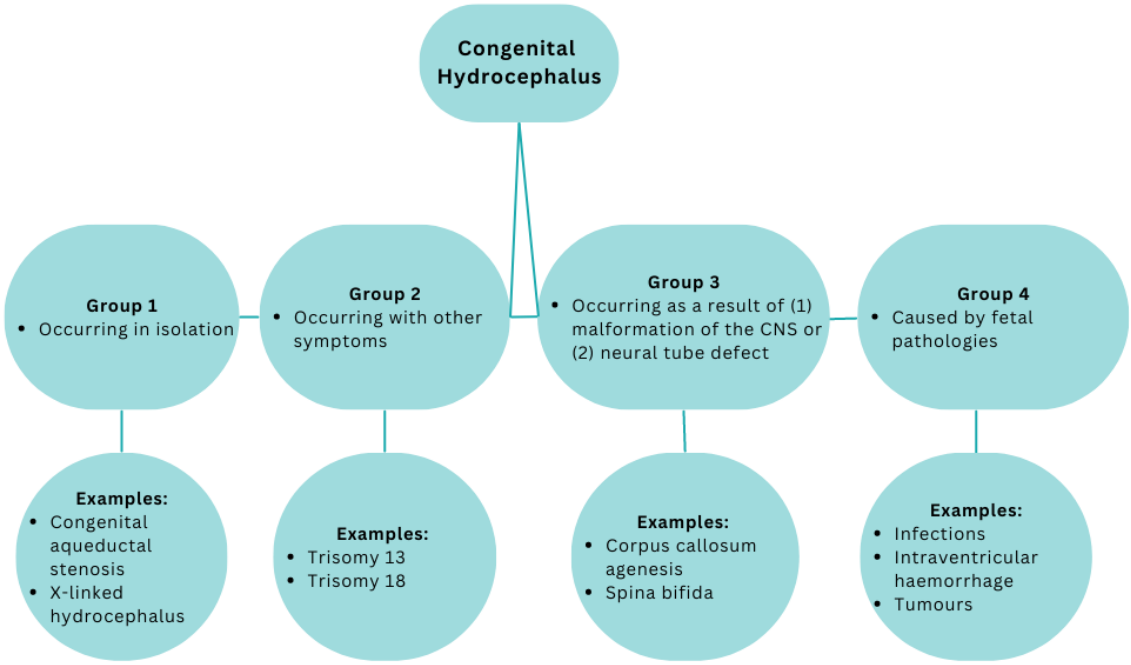

Figure 2.4: A flow chart showing the different groups of congenital hydrocephalus.

2.3.1.3a) Clinical presentation

In infants, aged 2 - 12 months, the following clinical presentations will be observed: the head circumference appearing to be increasing abnormally, vomiting, irritability, anterior fontanelle bulging, sun-setting eyes or cranial sutures spreading (Kahle *et al.*, 2016; Pisapia *et al.*, 2017). In young children, aged 1 – 4 years, it will present as headaches, vomiting, papilloedema, diplopia or developmental milestone loss (Kahle *et al.*, 2016; Pisapia *et al.*, 2017).

2.3.1.3b) Diagnosis

Various imaging techniques such as MRI and computed tomography (CT) may be used as standard diagnostic tools of diagnosis and to study ventricular dilation (Kahle *et al.*, 2016; Pisapia *et al.*, 2017). Usually, when an infant presents with an open fontanelle, cranial ultrasonography is used as an imaging method, however, an MRI scan is considered a better option as it can provide detailed information regarding the anatomy and the cause of hydrocephalus (Kahle *et al.*, 2016; Pisapia *et al.*, 2017).

As mentioned previously, communicating hydrocephalus, a type of chronic hydrocephalus, leads to the enlargement of the entire ventricular system (Leinonen *et al.,* 2018; Yin *et al.,* 2021). In contrast, non-communicating chronic hydrocephalus encompasses other types where only the paired lateral ventricles and the third ventricle experience enlargement (Bianchi *et al.*, 2021; Green *et al.*, 2021).

2.3.2 Non-communicating chronic hydrocephalus

Non-communicating hydrocephalus may be caused by multiple pathologies at different locations within the ventricular system (Greitz, 2004; Leinonen *et al.,* 2018). More so at locations such as the interventricular foramen and cerebral aqueduct, where the space for flow is narrower than in other locations in the system (Leinonen *et al.,* 2018; Farb and Rovira, 2020).

There are two types of non-communicating chronic hydrocephalus, namely: long-standing overt ventriculomegaly (LOVA) in adults and late-onset idiopathic aqueduct stenosis. These types are both known as triventricular hydrocephalus as they only affect the paired lateral and third ventricles (Bianchi *et al.*, 2021; Green *et al.*, 2021).

2.3.2.1 Long-standing overt ventriculomegaly in adults

Long-standing overt ventriculomegaly in adults (LOVA) is a type of non-communicating chronic hydrocephalus that is caused by congenital aqueduct stenosis (Oi *et al.*, 2000; Ved *et al.,* 2017). It progresses in an individual over a long period, therefore, the clinical presentations do not manifest at the onset of the disorder (Ibáñez-Botella *et al.*, 2017; Tuniz *et al.*, 2021). LOVA begins during infancy just before the cranial sutures close and remains compensated while the individual is asymptomatic or only displaying a few symptoms (Ibáñez-Botella *et al.*, 2017; Tuniz *et al.*, 2021).

2.3.2.1a) Clinical presentation

LOVA presents as supratentorial ventriculomegaly (Figure 2.5) and macrocephaly and individuals with the condition will have heads that are two standard deviations larger than their peers (Al-Jumaily *et al.*, 2012; Ibáñez-Botella *et al.*, 2017; Ved *et al.,* 2017). Macrocephaly serves as the main clinical feature of LOVA and distinguishes it from other types of chronic hydrocephalus (Al-Jumaily *et al.*, 2012; Tuniz *et al.*, 2021).

2.3.2.1b) Diagnosis

Oi *et al.,* (2000) diagnosed LOVA with the assistance of criteria that they established, which utilised two radiological features and one clinical feature. The radiological features are overt ventriculomegaly of the lateral and third ventricles with evidence of obliterated cortical sulci. The second radiological feature is that of a destroyed or enlarged sella turcica (Ibáñez-Botella *et al.*, 2017; Tuniz *et al.*, 2021).

The clinical feature is macrocephaly with the following symptoms present or absent: Hakim's triad of symptoms, headaches, parkinsonism, vegetative state, limited IQ, apathetic consciousness, and akinetic mutism (Al-Jumaily *et al.*, 2012; Ibáñez-Botella *et al.*, 2017; Ved *et al.,* 2017). These features, in conjunction with an Evan's Index of more than 0.4, are used to diagnose LOVA. Patients who present with ventriculomegaly and one of the other features will be diagnosed with LOVA (Ibáñez-Botella *et al.*, 2017; Tuniz *et al.*, 2021).

According to Ibáñez-Botella *et al.,* (2017) and Tuniz *et al.,* (2021), ventriculomegaly of the lateral and third ventricles is the most crucial diagnostic feature of LOVA and while aqueduct stenosis plays an important role as well, its absence cannot be used to exclude a person from being diagnosed with LOVA.

There is an agreement in the literature that LOVA is known as a triventricular hydrocephalus (Ved *et al.,* 2017; Bianchi *et al.*, 2021), however, Ibáñez-Botella *et al.,* (2017) suggested that LOVA could occur as either communicating or non-communicating depending on whether aqueduct stenosis is present or not. This was determined by observing the cranial MRI of CSF flow in the region of the aqueduct (Ibáñez-Botella *et al.*, 2017). However, few of the literature describes LOVA as non-communicating (Leinonen *et al.,* 2018; Tuniz *et al.*, 2021).

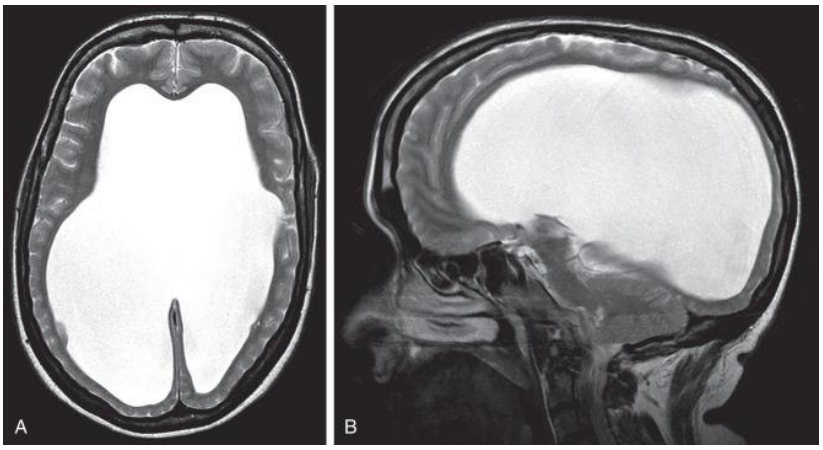

Figure 2.5: An image showing a patient with LOVA. (A) Axial T2 and (B) sagittal MRI scan of a patient with LOVA (Toma, 2000). Copyright 2018 by Elsevier.

2.3.2.2 Late-onset idiopathic aqueduct stenosis

This type of triventricular hydrocephalus also has a late onset with an intracranial pressure of <10-15 mmHg (Fukuhara and Luciano, 2001; Panigrahi *et al.*, 2021; Tuniz *et al.*, 2021). It occurs as a result of obstruction of the cerebral aqueduct, causing a decrease in CSF flow through the aqueduct (Locatelli *et al.*, 2014). This obstruction may be due to lesions (e.g. pineal tumours) or primitive stenosis (Locatelli *et al.*, 2014; Tuniz *et al.*, 2021).

2.3.2.2a) Clinical presentation

Young patients will present with headaches and older patients will present with symptoms from the NPH triad of symptoms (Locatelli *et al.,* 2014). Some patients may experience seizures and blurred vision, together with headaches or NPH symptoms (Fukuhara and Luciano, 2001).

2.3.2.2b) Diagnosis

In a study by Fukuhara and Luciano (2001), to aid in the diagnosis of late-onset idiopathic aqueduct stenosis (LIAS), they determined the Evans index and measured the width of the third ventricle. These values informed them of the extent of ventriculomegaly (Fukuhara and Luciano, 2001). Furthermore, CSF flow was studied using the cine phase-contrast MRI to verify the decreased flow through the cerebral aqueduct and they found that it was especially valuable in mild ventriculomegaly (Fukuhara and Luciano, 2001; Locatelli *et al.*, 2014). In addition to studying CSF flow, macroscopical obstruction of the aqueduct is another feature to look out for (Burtscher *et al.*, 2003). Although challenging to quantify, a small fourth ventricle was also used in diagnosis (Fukuhara and Luciano, 2001; Burtscher *et al.*, 2003).

It is evident from the literature that chronic hydrocephalus has different causative factors, even so, the clinical symptoms and the changes in its neuropathology are similar (Edwards *et al.*, 2004; Filis *et al.,* 2017). Although symptoms are similar across the different types of hydrocephalus, some types may manifest without certain symptoms. For example, cognitive

impairment may not always be present in iNPH (Edwards *et al.*, 2004), while macrocephaly is a key feature of LOVA (Tuniz *et al.*, 2021). Furthermore, there is a relationship between clinical symptoms and radiological features according to the literature, even asymptomatic patients have been found to display a few features during clinical diagnoses (Kockum *et al.*, 2018; Capone *et al.,* 2020).

Clinical diagnoses are strongly supported by computed tomography (CT) or MRI scans, as they aid in reducing differential diagnoses (Damasceno, 2015; Roblot *et al.*, 2021). Chronic hydrocephalus should not be suspected based only on cerebral imaging, however, it is essential for there to be clinical manifestations to determine a diagnosis (Roblot *et al.*, 2021). Moreover, if the ventricles are enlarged while there is no evidence of increased intracranial pressure or clinical manifestations radiologically, that warrants a possible diagnosis of non-active (arrested) hydrocephalus and should be investigated further (Edwards *et al.*, 2004).

2.4 Imaging

While both MRI and CT are recommended, using MRI in hydrocephalus cases helps to identify successive morphological arrangements (Kitagaki *et al.*, 1998; Roblot *et al.*, 2021). Moreover, MRI scans are ideal because they provide ample information required to eliminate other causes (Yin *et al.,* 2021). The higher imaging fidelity of MRI allows for the detection of subtle pathologies that may not be seen on CT, as well as better visualisation of the ventricle morphology.

The criteria for diagnosing iNPH using an MRI scan utilises two internationally recognised guidelines, namely: the Japanese guidelines and the American-European guidelines, where the latter is frequently used outside of Japan (Kockum *et al.*, 2018; Capone *et al.,* 2020; Nakajima *et al.*, 2021; Roblot *et al.*, 2021; Yin *et al.,* 2021). In addition to those guidelines, Kockum *et al.,* (2018) established a grading scale known as the Radscale, which was used to grade the radiological features of iNPH and assess their correlation to clinical symptoms. The authors also used the same clinical features that are found in the previously mentioned guidelines (Kockum *et al.,* 2018; Kockum *et al.,* 2019). However, these clinical features are not unique to iNPH as they are classical features of other chronic hydrocephalus types, and they are discussed in 2.4.1 (Hong *et al.*, 2016; Farb and Rovira, 2020).

2.4.1 Clinical features

2.4.1.1 Evans index

Evans index (≥ 0.3) is a radiological definition of ventriculomegaly, characterised by the widening of the ventricles and enlargement of the frontal horns of the lateral ventricles, with no evidence of cerebral atrophy (Damasceno, 2015; Roblot *et al.*, 2021). The index is a ratio of the maximum width across the frontal horns (blue line) and the maximum width of the inner plate of the cranium (red line), both on the same transverse slice (Kockum *et al.*, 2018) at the frontal horn level (Damasceno, 2015) seen in Figure 2.6.

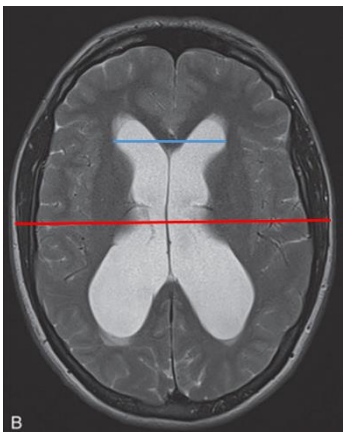

Figure 2.6: (B) Axial T2 sequence MRI scan of a patient showing ventriculomegaly (Toma, 2018). Copyright 2018 by Elsevier.

2.4.1.2 Temporal horns

Wide temporal horns encircled blue in Figure 2.7, are an indication of enlarged lateral ventricles in hydrocephalus patients, however, this width is not a consequence of hippocampal atrophy (Roblot *et al.*, 2021). The width of the horns will be ≥6 mm according to the literature (Virhammar *et al.*, 2014; Yin *et al.,* 2021). However, in a study by Andersson *et*

al., (2017), the limit was determined as ≥4 mm (Andersson *et al.,* 2017). Additionally, Kockum *et al.,* (2018) found that sensitivity and specificity were higher at a diameter of 4 mm, whereas they were low at 6 mm and that is the reason why they also chose a limit of 4 mm.

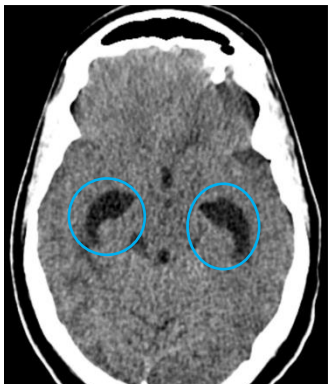

Figure 2.7: A CT scan of the brain in the coronal view, indicating the third ventricle shape. Image taken from the GSH PACS (20 October 2023).

2.4.1.3 Third ventricle

The third ventricle when viewed in the coronal plane, as seen in Figure 2.8, has walls that have a more convex shape, rather than a concave shape. This is also a morphological change that can be used when diagnosing chronic hydrocephalus (Capone *et al.,* 2020; Yin *et al.,* 2021).

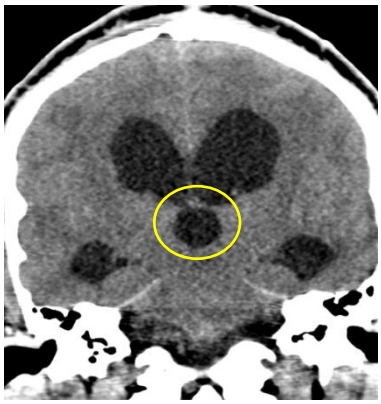

Figure 2.8: A CT scan of the brain in the coronal view, indicating the third ventricle shape. Image taken from the GSH PACS (20 October 2023).

2.4.1.4 Sylvian fissures

The Sylvian fissures are the CSF spaces that are bounded by the frontoparietotemporal operculum and the insular laterally (Kitagaki *et al.*, 1998). In CCH, they widen in the coronal plane (Figure 2.9, circled in green) (Kockum *et al.*, 2018), together with subarachnoid cisterns, while the cortical sulci and the higher convexity subarachnoid spaces appear narrower (Damasceno, 2015; Nakajima *et al.*, 2021; Roblot *et al.*, 2021). These are good indicators of damaged CSF dynamics within the subarachnoid space (Nakajima *et al.*, 2021).

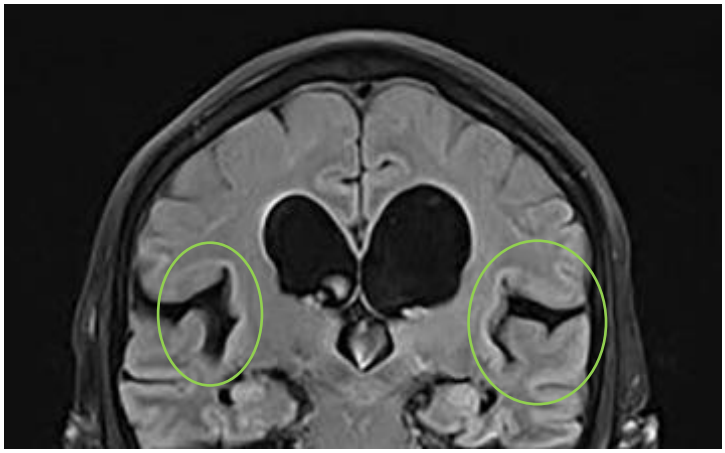

Figure 2.9: Coronal T2 MRI scan of a normal pressure hydrocephalus patient with dilated Sylvian fissures (Toma, 2018). Copyright 2018 by Elsevier.

2.4.1.5 Corpus callosum and callosal angle

The callosal angle, the angle between the lateral ventricles indicated by the arrow in Figure 2.10, can also be used as a marker of chronic hydrocephalus. Roblot *et al.,* (2021) and Damasceno (2015) state that patients with hydrocephalus will have an angle between 40 - 90^{o}, whereas healthy and elderly (those with brain atrophy) individuals will have angles between 100 - 120^{o} (Roblot *et al.*, 2021; Yin *et al.,* 2021).

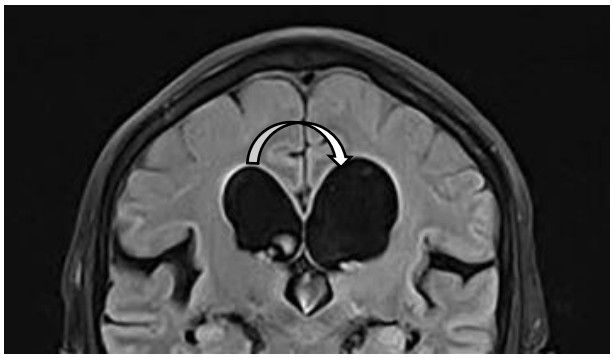

Figure 2.10: Coronal T2 MRI scan of a normal pressure hydrocephalus patient with narrow callosal angle (Toma, 2018). Copyright 2018 by Elsevier.

2.4.1.6 Periventricular white matter

The periventricular white matter changes, this change is not caused by demyelination, but rather by subcortical vascular encephalopathy present in patients with severe hydrocephalus (Damasceno, 2015; Engel *et al.*, 2021; Nakajima *et al.*, 2021). Moreover, periventricular white matter changes will result in signal changes on the MRI scan as seen in Figure 2.11 (Damasceno, 2015). Patients will present with frequent and wider periventricular and deep white matter hyperintensities, suggesting chronic cerebral ischemia (Roblot *et al.*, 2021).

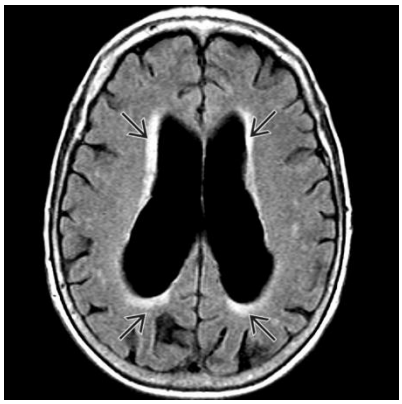

Figure 2.11: Axial flair MR shows enlarged ventricles out of proportion to the sulcal enlargement, with evident periventricular hyperintensity (indicated by the black arrows) (Osborn and Digre, 2016). Copyright 2016 by Elsevier.

Although the abovementioned criteria have been established, the implications surrounding the decision to perform surgery based on the criteria have been under scrutiny and have led to controversial results (Roblot *et al.*, 2021).

Among patients over the age of 60 years, approximately 6.5% have ventriculomegaly, however, it is important to note that a range of 0.1-0.5% of these patients present with iNPH thereby emphasising the inadequacy of relying solely on diagnostic imaging criteria for

accurate diagnosis (Roblot *et al.*, 2021). Furthermore, even though these criteria have been established, they are not considered standard (Yin *et al.,* 2021). Nonetheless, the clinical features mentioned in the criteria are seen in research studies and there is an agreement among researchers that these features do support the diagnosis of hydrocephalus (Kartal and Algin, 2014; Roblot *et al.*, 2021). While using MRI or CT scans to assess the presence of hydrocephalus is sufficient, ICP measurements may help with confirming chronic hydrocephalus (Panigrahi *et al.*, 2021).

2.5 Intracranial pressure measuring

Components of the central nervous system (CNS), namely: the brain, neurovascular structures, spinal cord, and CSF are contained within the inflexible skull and vertebral canal. The fused skull houses a sum volume of 1450mL, of which 1300mL is from the brain, 110mL from the blood and 65mL from CSF (Rangel-Castillo *et al.,* 2008). Moreover, the Monro-Kellie doctrine states that "the sum of volumes of blood, brain, CSF, and other components is constant and that an increase in any one of these must be offset by an equal decrease in another." According to this doctrine, if one of the other components does not decrease in volume, then the ICP will increase (Edwards *et al.*, 2004; Rangel-Castillo *et al.,* 2008).

Intracranial pressure measuring and monitoring are used to assess the changes in intracranial volume and thus help in the diagnosis of health issues that are associated with CSF dynamics (Evensen and Eide, 2020). That is why ICP measuring and monitoring are used to confirm chronic hydrocephalus (Evensen and Eide, 2020; Panigrahi *et al.*, 2021). To determine whether or not the increase in ICP is indicative of hydrocephalus, it is important to know the

normal ranges of ICP (Table 2.1), particularly because they differ with age (De Onis *et al.*, 2006; Rangel-Castillo *et al.,* 2008).

Table 2.1: Intracranial pressure measurements and the degree of severity of intracranial hypertension in relation to age. Adapted from De Onis *et al.,* (2006); Rangel-Castillo *et al., (*2008).

	Intracranial pressure	Age groups
Normal values	<2 mmHg	Neonates (0-1 months)
	1.5 – 6 mmHg	Term infants (2 – 12 months)
	3 – 7 mmHg	Young children (2 – 4 years)
	< 10 – 15 mmHg	Older children (5 – 12 years), adults (> 18 years)
Upper limit	15 – 20 mmHg	Older children (5 – 12 years), adults (> 18 years)
Mild intracranial hypertension	20 – 30 mmHg	
Requiring urgent treatment	> 20 – 25 mmHg	
Life-threatening intracranial hypertension	> 40 mmHg	

Differentiating between the different kinds of hydrocephalus is also done so successfully by measuring ICP, where the different hydrocephalus will have different ICP as seen in Table 2.2 (Panigrahi *et al.*, 2021).

Table 2.2: Intracranial pressure measurements of different types of hydrocephalus. Adapted from Panigrahi *et al.,* (2021).

Type of hydrocephalus	**Intracranial pressure**
No hydrocephalus	< 5 – 10 mmHg
Late-onset idiopathic aqueduct stenosis	< 10 – 15 mmHg
Normal pressure hydrocephalus	< 20 mmHg
Active hydrocephalus	Mean < 12 mmHg
Arrested hydrocephalus	Mean ≤ 12 mmHg
Compensated hydrocephalus	Mean ≤ 12 mmHg (with A and B waves)

Unfortunately, measuring ICP is a very invasive procedure, because it relies on neurosurgical expertise (Figures 2.12 & 2.13), and the procedure puts the brain of a patient at risk of

infection or haemorrhage (Evensen and Eide, 2020; Panigrahi *et al.*, 2021). Nonetheless, a successful diagnosis is necessary to decide on a treatment plan (Jaraj *et al.,* 2017).

Figure 2.12: An illustration of an intraparenchymal microtransducer, Triple Bolt, on a patient during ICP monitoring (Robba, 2018). Copyright 2018 by Elsevier. A – anterior, R – right side, P – posterior, L – left.

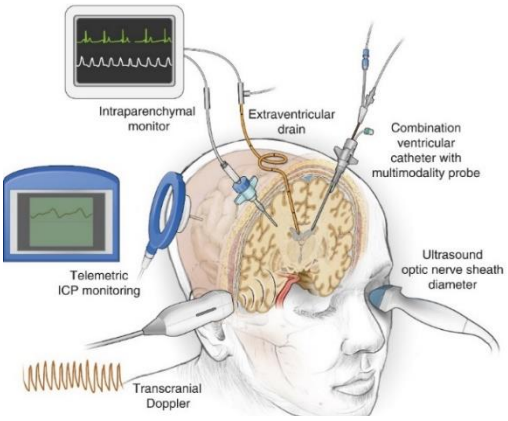

Figure 2.13: An illustration of the current intracranial pressure monitoring technology (DiGiorgio *et al.,* 2023). Copyright 2023 by Elsevier.

2.6 Treatment of chronic hydrocephalus

Treatment of hydrocephalus is crucial, particularly in the early stages of the disorder, because early treatment is more effective (Agarwal *et al.,* 2016; Andersson *et al.*, 2019; Green *et al.*, 2021). Patients who undergo treatment may experience improved symptoms (Capone *et al.,* 2020). Moreover, differential diagnosis is important when establishing a treatment, because their presence may affect the outcome of the treatment (Jaraj *et al.*, 2017; Leinonen *et al.,* 2018; Roblot *et al.*, 2021).

The well-known approach for treating communicating chronic hydrocephalus through surgical intervention is by diverting CSF using CSF shunts, and this form of treatment has a response rate of 50-60% (Kartal and Algin, 2014; Dewan *et al.*, 2018). These shunting devices are intraventricular and they drain excess fluid into another compartment in the body,

depending on the type of shunt used ventriculoperitoneal shunts drain CSF from the ventricle and into the peritoneal cavity (Roblot *et al.*, 2021).

When it comes to triventricular (non-communicating chronic) hydrocephalus, endoscopic third ventriculostomy (ETV) is the first option for treatment (Locatelli *et al.*, 2014; Bianchi *et al.*, 2021). ETV is highly successful in treating hydrocephalus in many patients, however, it is susceptible to failing early, and this is especially evident in infants (Kahle *et al.*, 2016). Upon failure of ETV, a ventriculoperitoneal (VP) shunt with a gravitational valve will be inserted (Ibáñez-Botella *et al.*, 2017; Tuniz *et al.*, 2021). These shunts need to have valve mechanisms that regulate flow combined with gravitational devices, this will help prevent over-drainage (Kahle *et al.*, 2016; Tuniz *et al.*, 2021).

2.7 Conclusion

Hydrocephalus is a common CNS disorder that, left untreated can have detrimental effects on cerebral structures. Acute hydrocephalus can lead to raised intracranial pressure, coma and even death. Chronic hydrocephalus can cause a debilitating decline in neurocognitive and visual function. CSF diversion of any form of active hydrocephalus will ensure better neurological functioning for the patient. However, when treated early, a CSF shunt or the ETV procedure may improve symptoms. Therefore, correct, and early diagnosis is essential. There are criteria for specific cerebral and ventricular clinical features that can help with diagnosing chronic hydrocephalus, using MRI or CT scans. However, to confirm chronic hydrocephalus, invasive methods such as measuring ICP are currently being used and they can put the brain at risk of infection or haemorrhage. To try and reduce the number of patients who may have

to undergo surgery without the need and in addition to the clinical features described in the criteria established, the frontal horn shape described will be an added unique feature.

Chapter 3: Materials and Methods

3.1 Methodology

This was a retrospective, observational and quantitative study. The study examined the size and shapes of the ventricles and the CSF spaces in the brain scans of patients who had been diagnosed with hydrocephalus. Approval was obtained from the University of Cape Town (UCT) Faculty of Health Sciences Research Ethics Committee, Groote Schuur Hospital (GSH) Research Ethics Committee and the Radiology Department at GSH to access patient scans and records (3.6 Ethical considerations for relevant Appendices).

3.2 Methods

3.2.1 Setting

The study took place at the Radiology Department at GSH, studying patients who came in reporting symptoms associated with hydrocephalus, who were then examined with surveillance imaging. Consequently, these patients have had MRI or CT scans taken at GSH between 2017 – 2023. Those who were thought to have hydrocephalus further underwent surgery where ICP was reported.

3.3 Sampling

3.3.1 Sample selection

The study used a purposive sampling method, selecting patients who fit the study's criteria and who would meet the study's objectives. Medical records were reviewed to identify patients suspected of having hydrocephalus, or patients known to have hydrocephalus and have undergone surgery to measure the intracranial pressure. Furthermore, the participants were selected based on the inclusion and exclusion criteria (Table 3.1). Given the exploratory nature of our study, we chose a sample size of 150 participants.

3.3.2 Inclusion and exclusion criteria

Table 3.1: Inclusion and exclusion criteria for sample selection.

Inclusion criteria	**Exclusion criteria**
Age 17 years and older	
Experienced at least 2 symptoms associated with hydrocephalus (set by the Japanese guidelines (Nakajima *et al.*, 2021). Symptoms: • Headaches • Nausea • Vomiting • Blurred vision • Double vision • Changes in behaviour • Changes in consciousness • Seizures	Medical conditions affecting only brain parenchyma and not directly related to hydrocephalus. Excluded medical conditions: • Brain tumours • Intracerebral lesion haemorrhages • Subarachnoid haemorrhages • Traumatic brain injuries • Meningitis

3.4 Study population

Following the selection process, the final population consisted of 150 patients which included a group of patients with diagnosed hydrocephalus and a group of controls. The group consisting of hydrocephalus patients was then subdivided into acute and chronic groups.

The acute patients had objectively measured raised intracranial pressure (Bratton *et al.*, 2007), measured at the time of surgery, and was formally documented. This pressure was measured to shunt the ventricles, by lumbar puncture, or by invasive monitoring of ICP. The patients who had chronic hydrocephalus were those who had normal pressure measured by the same procedures as the acute patients.

Patients in the control group had been diagnosed with age-related brain atrophy following the differential diagnosis of hydrocephalus as the cause of ventricular enlargement. It was proven upon investigating their MRI or CT scans that they had “large ventricles” due to atrophy or white matter loss. This group was selected by keyword searching through medical records for terms such as “ex vacuo dilation”, and “age-related atrophy”.

The focus of this study was to compare these three groups, consisting of 50 patients each. The differentiation of these groups into acute and chronic hydrocephalus, as well as the control group, is illustrated in Figure 3.1.

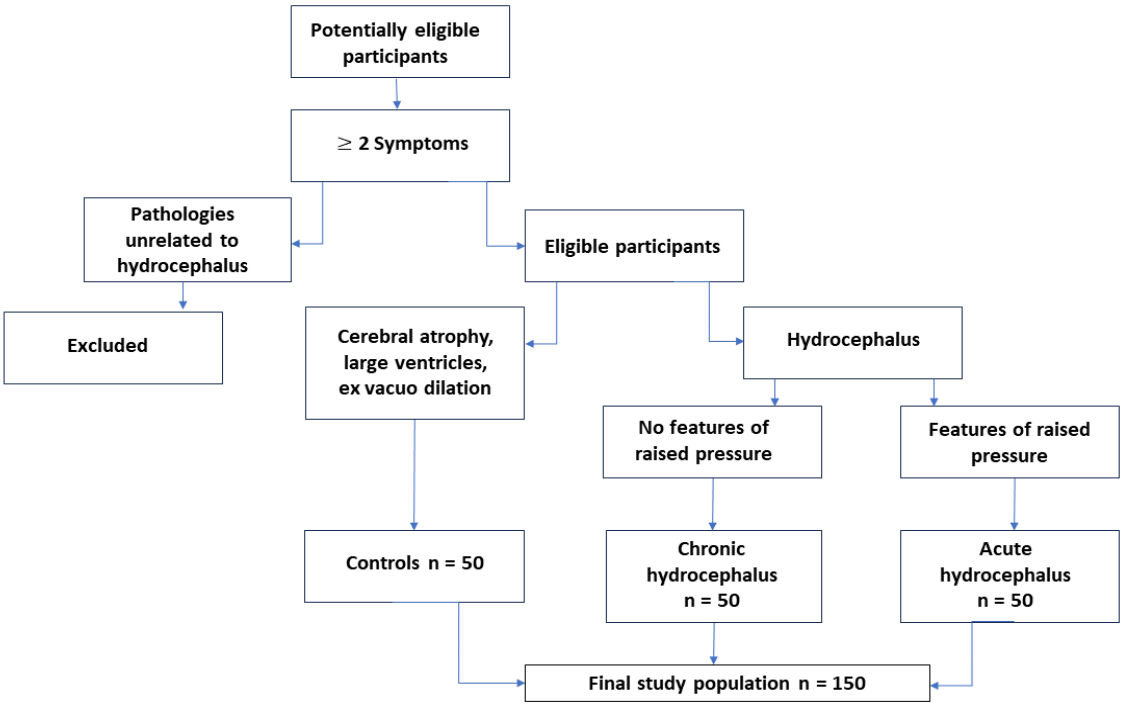

Figure 3.1: Population sampling.

3.5 Study procedure and outcomes

The hospital's Picture Archiving and Communication digital imaging System (PACS) was accessed for the (uncontrasted and contrasted) MRI and CT scans, as well as the demographic and clinical data.

The MRI and CT scans were observed for clinical features commonly found on the scans of hydrocephalus patients including, enlarged ventricular system and CSF spaces, periventricular white matter changes (PWMC) and narrowed callosal angles (CA), these features were then measured as described in 3.6.1. The features were measured from all three groups (chronic, acute and control), to later explore the measurement differences between these groups. All study data was stored in REDCap (Research Electronic Data Capture) software and access to the data was controlled.

3.5.1 Morphometrics

After consulting with a radiologist, the scans were viewed using the multiplanar reconstruction (MPR) display method. These scans had to be adjusted using reference lines to ensure the brain images were straight.

This was achieved in a stepwise method as follows:

- Step 1: The vertical line (red) in Figure 3.2 was placed in the midsagittal plane.

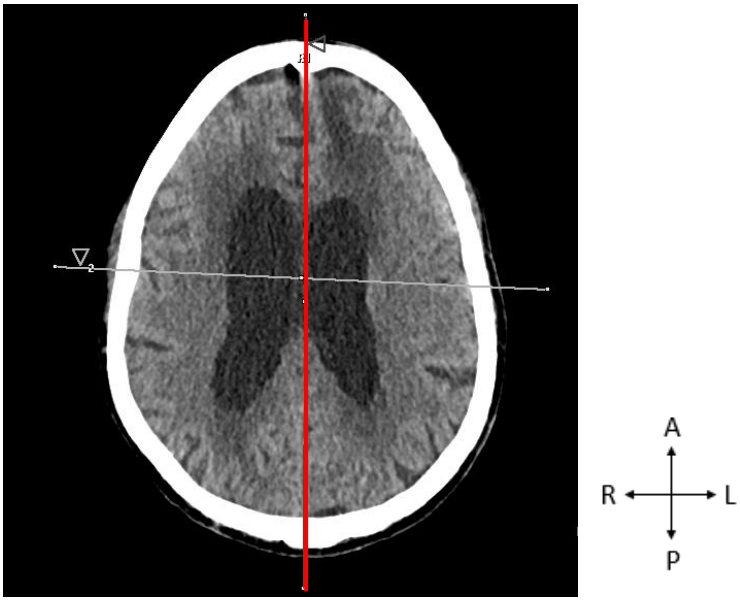

Figure 3.2: A CT scan showing the brain in the axial view indicating the midsagittal reference line (red). Image taken from the GSH PACS (20 October 2023). A - Anterior, R - Right, P - Posterior, L - Left.

- Step 2: The horizontal line (green) in Figure 3.3 was aligned with the inferior border of the foramen magnum, with the vertical line (blue) perpendicular to it.

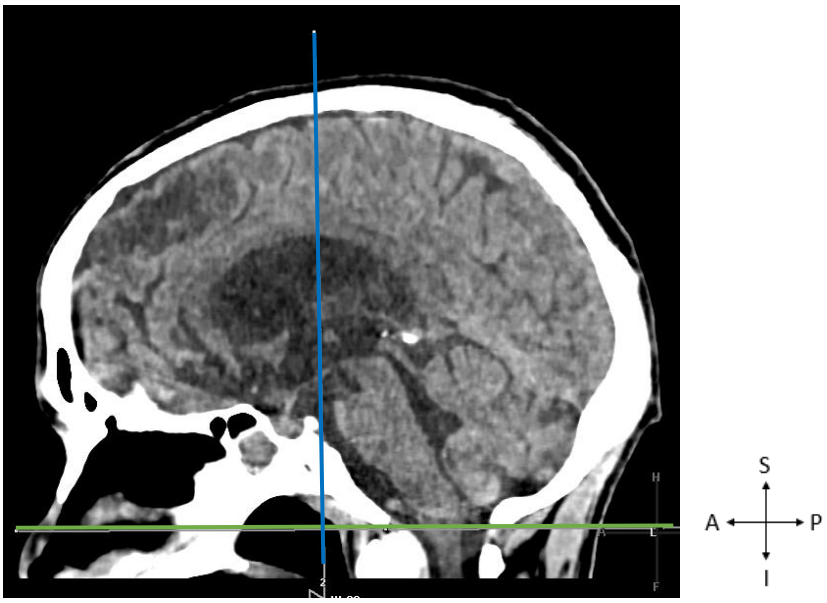

Figure 3.3: A CT scan showing the brain in the sagittal view indicating the reference line at the inferior border of the foramen magnum (green) and the reference line perpendicular to it (blue). Image taken from the GSH PACS (20 October 2023). S - Superior, A - Anterior, I - Inferior, P - Posterior.

- Step 3: The horizontal lines (orange) in Figures 3.4A & B were placed traversing the ear ossicles (encircled in orange) bilaterally.

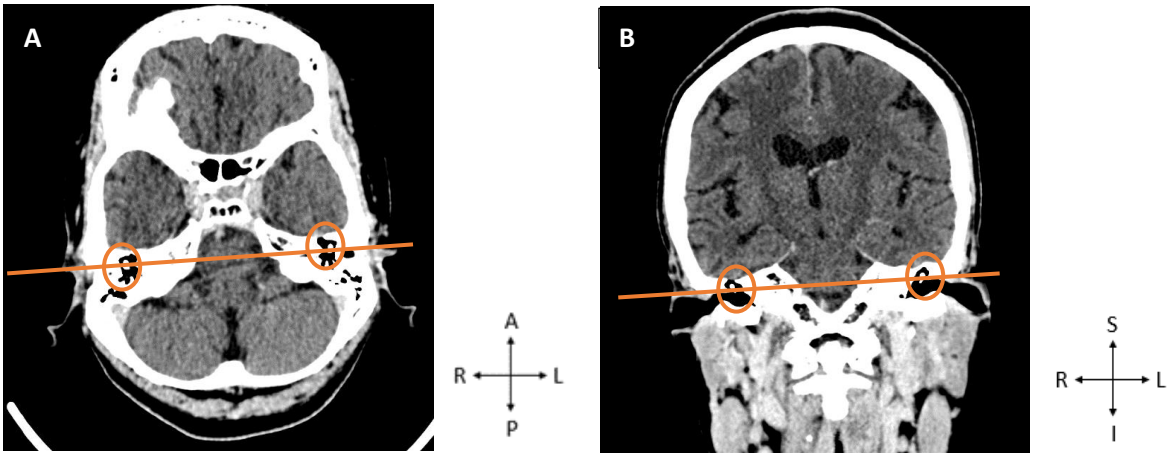

Figure 3.4: CT scans showing the brain in the axial view (A) and the coronal view (B), indicating the paired ear ossicles (encircled) with the reference lines (orange) traversing the ossicles. Image taken from the GSH PACS (20 October 2023). A - Anterior, R - Right, P - Posterior, L - Left, S - Superior, I - Inferior.

Once the brain was aligned, the morphometrics below were measured in millimetres (mm), using the ruler and angle functions within the PACS system to determine the features' size and describe their shape.

1. Evans index

   Method of measurement: The maximum width across the frontal horns (blue line) was divided by the maximum width of the inner cranial plate (red line), on the same axial plane shown in Figure 3.5 (Damasceno, 2015; Kockum *et al.*, 2018a). Multiple bifrontal measurements were taken across multiple slices to determine the maximum measurements. Once the maximum bifrontal width was established, the maximum width of the inner cranial plate was measured on the same transverse slice.

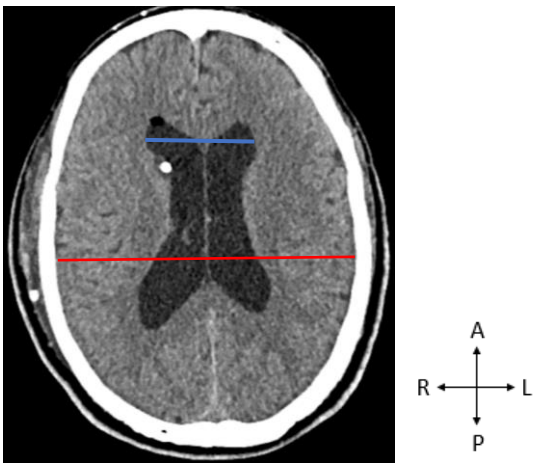

Figure 3.5: A CT scan of the brain in the axial view, indicating the bifrontal horn width (blue line) and the maximum inner cranial plate (red line). Image taken from the GSH PACS (20 October 2023). A - Anterior, R - Right, P - Posterior, L - Left.

2. Temporal horns

Method of measurement: Multiple measurements across the bilateral temporal horns were taken to get the bilateral maximum width in the axial plane, indicated in Figure 3.6 by orange lines (Kockum *et al.*, 2018).

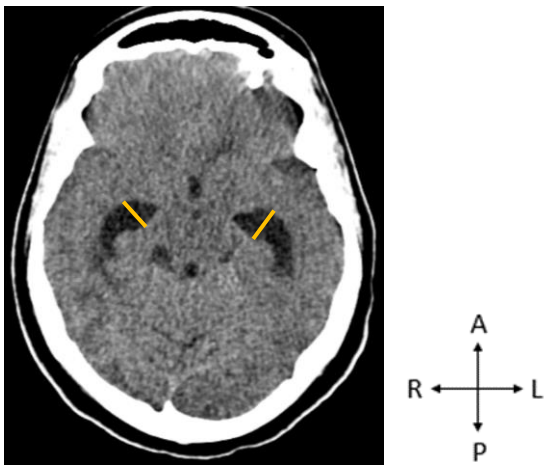

Figure 3.6: A CT scan of the brain in the axial view showing the temporal horn width, indicated by the orange lines. Image taken from the GSH PACS (20 October 2023). A - Anterior, R - Right, P - Posterior, L - Left.

3. Third ventricle

Method of measurement: The maximum width of the ventricle in the axial plane is indicated by the yellow line in Figure 3.7. This width will be determined after taking multiple measurements across the ventricle and different slices showing the third ventricle. The third ventricle shape, indicated within the orange circle in Figure 3.8, was described in the coronal plane (Capone *et al.,* 2020; Yin *et al.,* 2021).

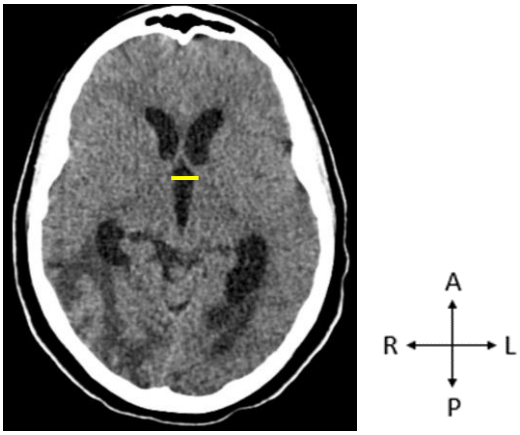

Figure 3.7: A CT scan of the brain in the axial view, indicting the third ventricle width. Image taken from the GSH PACS by (20 October 2023). A - Anterior, R - Right, P - Posterior, L - Left.

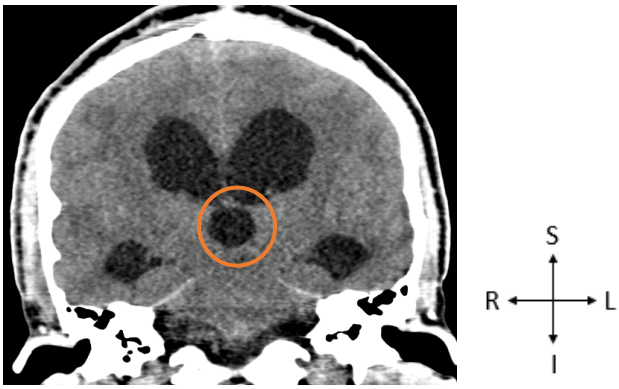

Figure 3.8: A CT scan of the brain in the coronal view, indicating the third ventricle shape. Image taken from the GSH PACS (20 October 2023). S - Superior, R - Right, I - Inferior, L - Left.

4. Callosal angle

Method of measurement: It was measured in between the lateral ventricles in the coronal plane, as indicated by the green lines in Figure 3.9. The coronal plane was at the level of the posterior commissure, with the plane orthogonal to the anterior-posterior commissure line (Damasceno, 2015). The CA was categorised into angles that represented patients who had hydrocephalus (40 - 90^{o}) as well as healthy and atrophied patients (100 - 120^{o}).

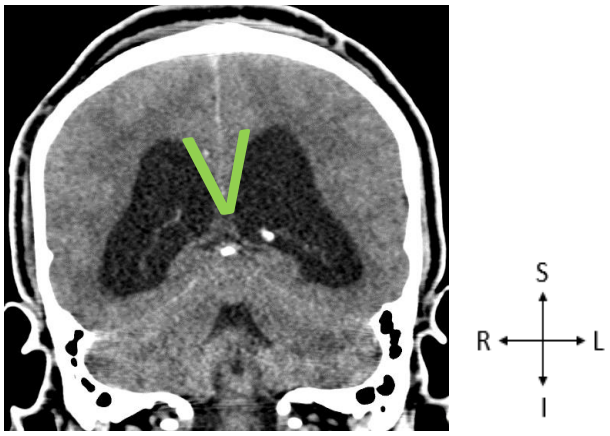

Figure 3.9: A CT scan of the brain in the coronal view indicating the callosal angle (green). Image taken from the GSH PACS (20 October 2023). S - Superior, R - Right, I - Inferior, L - Left.

5. Frontal horns

In the axial plane, the frontal horns were examined, and their shape was described. The shape was described as either round (blue line) in Figure 3.10 or quadrilateral (red line) in Figure 3.11 at the level of the anterior and posterior commissure.

Round/Oval: the tip of the frontal horn appears round, and the angle in between the horns is acute. Quadrilateral: the angle between the horns appears obtuse, and the horns take on a more square/quadrilateral shape.

Furthermore, the ICP was recorded as low-moderate and high according to the medical records, and its association with the frontal horn shape was then evaluated.

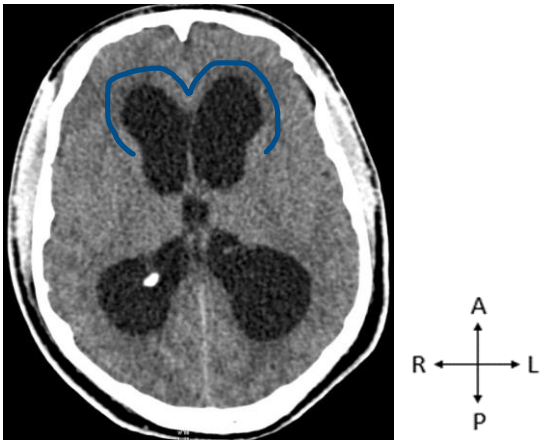

Figure 3.10: A CT scan of the brain in the axial view indicating the round frontal horn shape (blue). Image taken from the GSH PACS (20 October 2023). A - Anterior, R - Right, P - Posterior, L - Left.

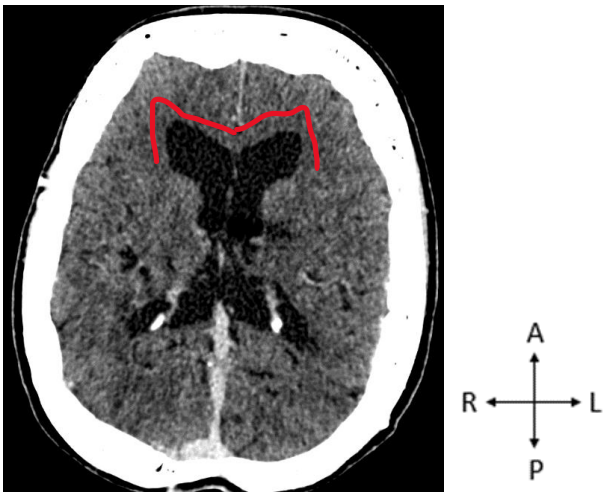

Figure 3.11: A CT scan of the brain in the axial view indicating the quadrilateral frontal horn shape (red). Image taken from the GSH PACS (20 October 2023). A - Anterior, R - Right, P - Posterior, L - Left.

6. Sylvian fissures

Method of measurement: Multiple measurements of the bilateral fissures were taken in the coronal plane, where the maximum height and width, indicated by the blue arrows in Figure 3.12 were measured. Measurements were taken where the sylvian fissures appeared to be the widest (Damasceno, 2015).

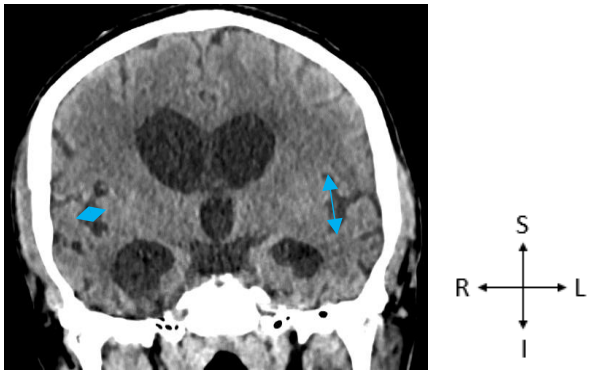

Figure 3.12: A CT scan of the brain in the coronal view indicating the Sylvian fissure width (left blue arrow) and height (right blue arrow). Image taken from the GSH PACS (20 October 2023). S - Superior, R - Right, I - Inferior, L - Left.

7. Periventricular white matter

Were defined as not present, present around frontal and/or temporal horns or spread around lateral ventricles, in the transverse plane as indicated in Figure 3.13 (Kockum *et al.*, 2018; Engel *et al.*, 2021).

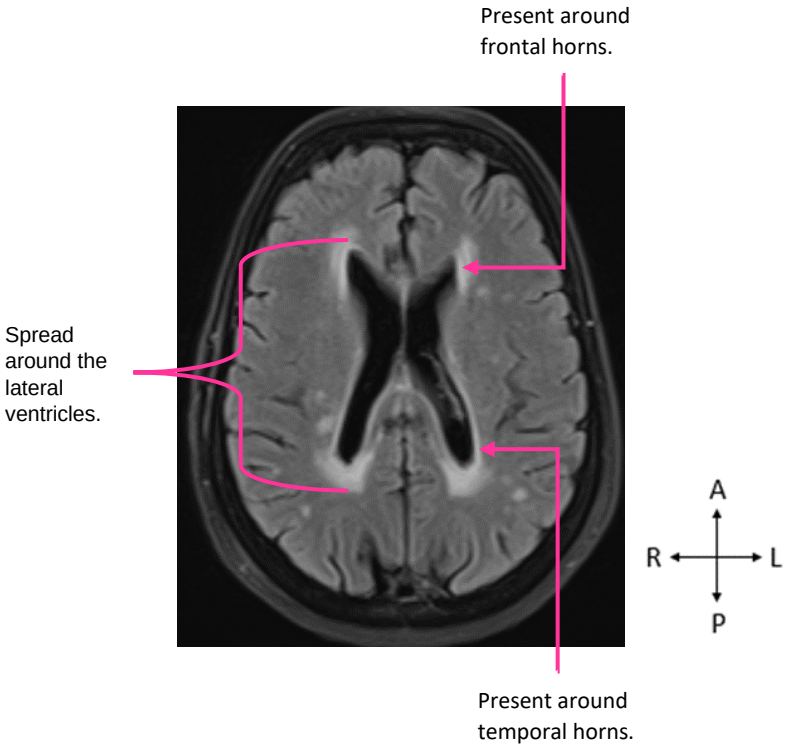

Figure 3.13: An MRI scan of the brain in the axial view indicating periventricular white matter changes. Image taken from the GSH PACS (20 October 2023). A - Anterior, R - Right, P - Posterior, L - Left.

3.6 Data management plan

All study data obtained from the hospital's PACS system was entered into a datasheet and transferred into REDCap software. The Data Management Plan is attached in Appendix A. Quality control included 100% double data entry by the researcher. An independent observer checked 20% of the data transferred from the datasheet to REDCap.

3.7 Study reliability

Reliability was monitored by a second observer who carried out 20% of the PACS measurements, in the same manner as data collection. The second observer was trained by the researcher on how to operate the PACS system. For intra-observer reliability, measurements were repeated twice. These repeated measurements were necessary to increase validity, and they were taken on two separate occasions. Both observers evaluated the scans and took measurements independently.

3.8 Statistical analysis

3.8.1 Quantitative data

RStudio (version 4.1.3) was used to analyse the quantitative and categorical data.

The Shapiro-Wilks test was used to test if the quantitative data was normally distributed. The quantitative data was described using medians and interquartile ranges (IQR), due to

the non-normal distribution of the data. The relationship between the quantitative variables and the group (chronic, acute, and controls) was then examined using the Mann-Whitney U test (MU). To examine the validity and reliability of the collected numeric data, the interobserver data was analysed using the intraclass correlation test (ICC).

3.8.2 Categorical data

Categorial data was represented by frequency tables with counts and percentages in parentheses and a CI of 95%. To examine the relationship between the categorical variables and the groups (chronic, acute, and control), variables were analysed using Fischer's Exact (F) and Chi-Square tests. The odds ratio (OR)was employed to investigate any correlation between the variables and the hydrocephalus diagnosis. The frontal horn shape interobserver data was analysed using intraclass correlation coefficient, to assess the degree of agreement between both observers. For Chi-square tests, the log likelihood ratio test, also known as the G-test in R was used where expected cell counts were less than required for the Pearson’s Chi-square test (McHugh, 2013).

3.9 Ethical consideration

Ethical approval was obtained from the Human Research Ethics Committee at both the University of Cape Town – Ethics reference number HREC REF 700-2022 (Appendix B) and Groote Schuur Hospital, and the Head of the Radiology Department at GSH (Appendix C). The study was carried out according to the Declaration of Helsinki ('World Medical Association Declaration of Helsinki: Ethical Principles for Medical Research Involving Human Subjects', 2013) and the South African Protection of Personal Information Act (POPIA) (*Protection of Personal Information Act (POPI Act)*, no date). All study data was de-identified to maintain patient confidentiality. Each patient's data was assigned a study number and is referenced as such in all written material.

Chapter 4: Results

4.1 Sample population

The total sample population of the study was 150, this population was then divided into three groups, namely, the chronic and acute hydrocephalus and control groups. Each group consisted of 50 patients, and because the sampling method was purposive, patients who fit the exclusion criteria were excluded at the beginning of the study. Of the 150 patients, 69 (46%) were female (23 – chronic, 20 – controls and 26 – acute) and 81 (54%) were male (27 – chronic, 30 – controls and 24 – acute), with ages ranging from 17 to 96 years.

For statistical analyses, the variables of age and sex were controlled to increase the strength of the predictability of the condition, either chronic or acute, as they were potential confounders. The results in Tables 4.1 and 4.2 below indicate that between the sex and age in all three groups, the only variable with a $p < 0.05$ was the difference in age distribution between the chronic HCP patients and the control group. Results with a $p < 0.05$ were considered to be significant.

Table 4.1: Differences in age and sex distributions between controls and chronic hydrocephalus groups.

	CON	CHCP	P value	Test
Age *[median (IQR) years]*	66.0 (49.0 – 74.5)	35.5 (29.0 – 45.0)	<0.001	MU
Sex *[% (n)female]*	40 (20)	46 (23)	0.689	F

Abbreviations: CHCP, Chronic Hydrocephalus; CON, Controls; F, Fisher's exact test; MU, Mann Whitney U test.

Table 4.2: Differences in age and sex distributions between chronic and acute hydrocephalus groups.

	CHCP	AHCP	P value	Test
Age *[median (IQR) years]*	35.5 (29.0 – 45.0)	40.0 (28.0 – 50.75)	0.326	MU
Sex *[% (n)female]*	46 (23)	52 (26)	0.689	F

Abbreviations: CHCP, Chronic Hydrocephalus; AHCP, Acute Hydrocephalus; F, Fisher's exact test; MU, Mann Whitney U test.

The data was then tested for normality. The Shapiro-Wilks test confirmed the non-normal distribution of the data from all three groups, chronic, acute and control, except for age between acute and chronic HCP patients (Appendix D). The non-normal distribution resulted in using the median and interquartile ranges for analyses, with a 95% confidence interval. Once the type of distribution was established, the clinical features were analysed using the appropriate statistical tests.

4.2 Clinical Feature Measurements

4.2.1 Evans Index (EI)

The EI was compared between the groups to see whether there was an association between the index and the presence of hydrocephalus (Tables 4.3 & 4.4 and Figure 4.1).

There was a significant difference in EI between the control and chronic HCP group ($p = 0.001$). The chronic HCP group had a high proportion (82%) of scans with an EI > 0.3, the control group almost had an equal proportion of scans with an EI < 0.3 (44%) and EI > 0.3 (56%) (Table 4.3).

Table 4.3: Evaluating differences in EI and the proportions of participants with EI >= 0.3 between the controls and chronic hydrocephalus groups.

	CON	CHCP	P value	Test
EI *[median (IQR)]*	0.3 (0.27 – 0.33)	0.35 (0.3 – 0.37)	0.001	MU
EI < 0.3 [n (%)]	22 (44)	9 (18)	0.009	F
EI > 0.3 *[n (%)]*	28 (56)	41 (82)		

Abbreviations: CHCP, Chronic Hydrocephalus; CON, Controls; CON, Controls; MU, Mann Whitney U test; F, Fisher's Exact.

Table 4.4 shows that there was no statistical significance between the EI between the chronic and acute HCP groups (p = 0.556). The proportion of the EI > 0.3 was almost equal between the chronic (82%) and acute (80%) HCP groups and the difference between them was not significant (p = 1.0).

Table 4.4: Evaluating differences in EI and the proportions of participants with EI >= 0.3 between the chronic and acute hydrocephalus groups.

	CHCP	AHCP	P value	Test
EI *[median (IQR)]*	0.35 (0.3 – 0.37)	0.34 (0.30 – 0.37)	0.556	MU
EI < 0.3 [n (%)]	9 (18)	10 (20)	1.0	F
EI > 0.3 *[n (%)]*	41 (82)	40 (80)		

Abbreviations: CHCP, Chronic Hydrocephalus; AHCP, Acute Hydrocephalus; MU, Mann Whitney U test; F, Fisher's Exact test.

Figure 4.1 illustrates the distribution of the EI data across all three groups, further showing the significant difference in the EI between the control and chronic HCP groups. The intraclass correlation coefficient (ICC) was excellent for all three groups: 0.981 in the control group, 0.986 in the chronic HCP group and 0.974 in the acute HCP group.

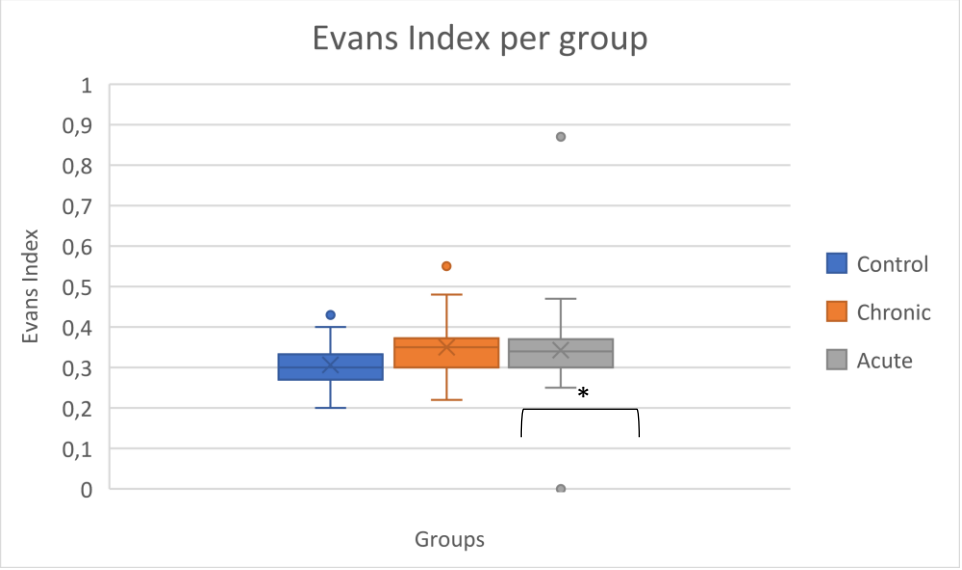

Figure 4.1: Boxplots showing the Evans Index of the three different groups. Indicating the maximum and minimum values, the first and third quartile, and the median. The outliers are represented as dots. * Indicates a significant difference, $p < 0.05$.

4.2.2 Temporal Horn Width

Both left and right temporal horn widths from the chronic HCP group were statistically significantly larger than those from the control group, p = 0.003 and 0.004, respectively (Table 4.5). The left temporal horn widths were larger than the right temporal horn widths.

Table 4.5: Differences in temporal horn width between the controls and chronic hydrocephalus groups.

	CON	CHCP	P value	Test
Width – Left *[median (IQR) mm]*	7.08 (4.61 – 9.4)	9.65 (6.65 – 14.21)	0.003	MU
Width – Right *[median (IQR) mm]*	6.83 (4.76 – 8.99)	8.48 (6.35 – 15.79)	0.004	MU

Abbreviations: CON, Controls; CHCP, Chronic Hydrocephalus; MU, Mann Whitney U test.

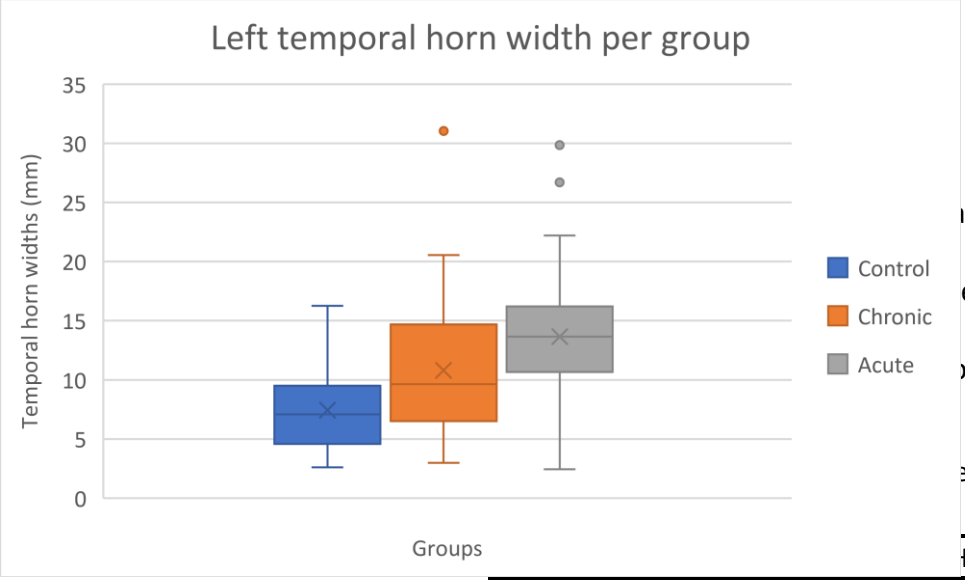

l horn widths between the acute

ely. The left temporal horn widths

oups.

e and chronic hydrocephalus groups.

		HCP	P value	Test
Width – Left *[median (IQR) mm]*	9.65 (6.65 – 14.21)	13.65 (10.80 – 16.07)	0.005	MU
Width – Right *[median (IQR) mm]*	8.48 (6.35 – 15.79)	13.03 (10.21 – 15.44)	0.02	MU

Abbreviations: CHCP, Chronic Hydrocephalus; AHCP, Acute Hydrocephalus; MU, Mann Whitney U test.

Figures 4.2 and 4.3 illustrate the distribution of the data across all three groups, indicating the significant difference in both the left and right temporal horn widths between the control and chronic HCP groups, as well as between the chronic and acute HCP groups.

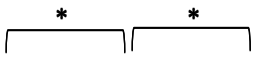

Figure 4.2: Left temporal horn widths across all three groups. Indicating the maximum and minimum values, the first and third quartile, and the median. The mean is represented by the (x), while the outliers are represented as dots. * Indicates the significant difference in temporal horn width, $p < 0.05$.

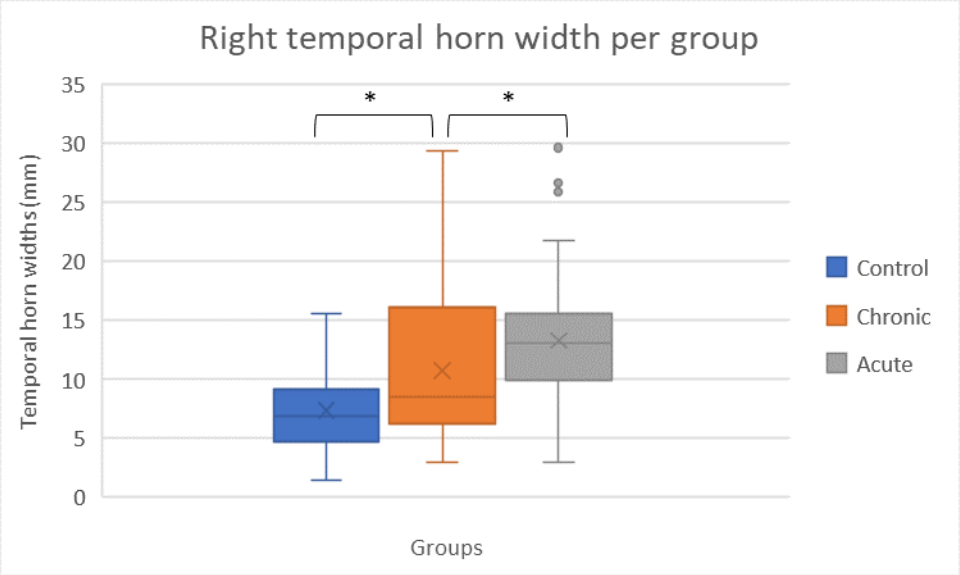

Figure 4.3: Right temporal horn widths across all three groups. Indicating the maximum and minimum values, the first and third quartile, and the median. The mean is represented by the (x), while the outliers are represented as dots. * Indicates the significant differences $p < 0.05$.

A comparison of controls and chronic HCP groups showed that > 58% of the data had temporal horn widths larger than 6.0mm in both groups and on both sides. This data was not statistically significant, $p > 0.05$ (Table 4.7).

Table 4.7: Evaluating the difference in proportions of participants with left temporal horn width > 6.0 between controls and chronic hydrocephalus groups.

		CON	CHCP	P value	Odds ratio	Test
Left	<= 6.0 [n (%)]	19 (38)	11 (22)	0.126	0.464	F
	> 6.0 [n (%)]	31 (62)	39 (78)			
Right	<= 6.0 [n (%)]	21 (42)	11 (22)	0.053	0.393	F
	> 6.0 [n (%)]	29 (58)	39 (78)			

Abbreviations: CON, Controls; CHCP, Chronic Hydrocephalus; F, Fisher's Exact test.

The data between the chronic and acute HCP also had the majority (> 78%), larger than 6.0mm, on both sides. The comparison of left temporal horn width between both groups was statistically significant (p = 0.041), unlike the data on the right (p = 0.171) (Table 4.8).

Table 4.8: Evaluating the difference in proportions of participants with left temporal horn width > 6.0 between the acute and chronic hydrocephalus groups.

		CHCP	AHCP	P value	Odds ratio	Test
Left	<= 6.0 [n (%)]	11 (22)	3 (6)	0.041	0.229	F
	> 6.0 [n (%)]	39 (78)	47 (94)			
Right	<= 6.0 [n (%)]	11 (22)	5 (10)	0.171	0.398	F
	> 6.0 [n (%)]	39 (78)	45 (90)			

Abbreviations: CHCP, Chronic Hydrocephalus; AHCP, Acute Hydrocephalus; F, Fisher's Exact test.

The ICC results of the left temporal horn width were as follows: the control and chronic groups had moderate reliability with ICCs of 0.512 and 0.747, respectively. The acute group had poor reliability with an ICC of 0.331. The ICC results of the right temporal horn width were as follows: the control group had poor reliability with an ICC of 0.298, the chronic group had good reliability with an ICC of 0.783 and the acute group had a negative ICC of 0.469.

4.2.3 Third Ventricle width and shape

There was a statistically significant difference in the third ventricle width between the controls and chronic HCP patients of 3.37mm, p < 0.001 (Table 4.9 and Figure 4.4). The

difference in median width of 0.30mm between the chronic and acute HCP groups was not statistically significant, p = 0.679 (Table 10 and Figure 4.4).

Table 4.9: Differences in third ventricle width between the controls and chronic hydrocephalus groups.

	CON	CHCP	P value	Test
Width *[median (IQR) mm]*	9.03 (6.76 – 11.48)	12.4 (8.79 – 15.08)	<0.001	MU

Abbreviations: CON, Controls; CHCP, Chronic Hydrocephalus; MU, Mann Whitney U test.

Table 4.10: Differences in third ventricle width between the acute and chronic hydrocephalus groups.

	CHCP	AHCP	P value	Test
Width *[median (IQR) mm]*	12.4 (8.79 – 15.08)	12.70 (9.85 – 14.96)	0.679	MU

Abbreviations: CHCP, Chronic Hydrocephalus; AHCP, Acute Hydrocephalus; MU, Mann Whitney U test.

The graphical representation of the third ventricle widths (Figure 4.4), where a distinct and significant difference can be seen between the control and chronic HCP groups (p < 0.001). The difference between the chronic and acute HCP groups was not significant (p = 0.679).

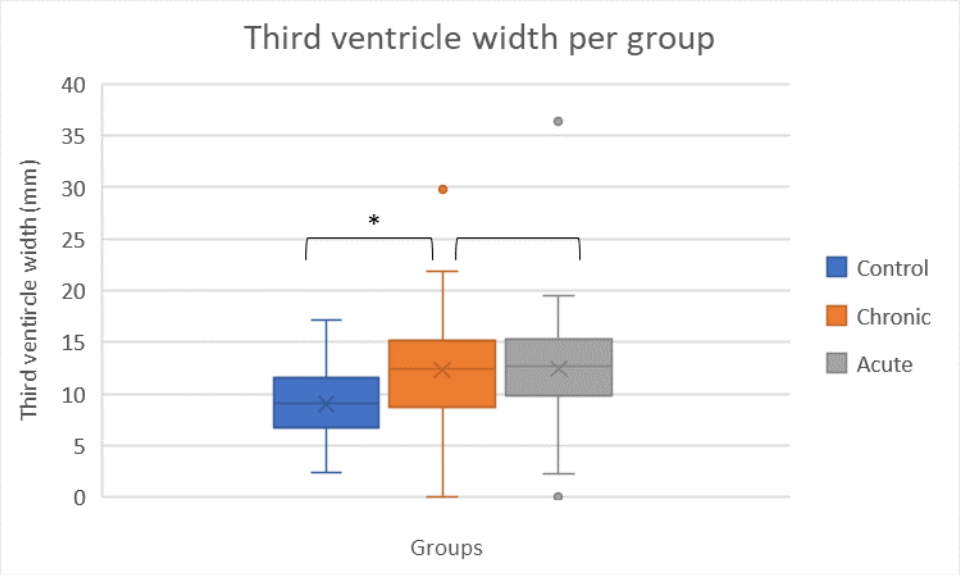

Figure 4.4: Third ventricle width across all three groups. Indicating the maximum and minimum values, the first and third quartile, and the median. The mean is represented by the (x), while the outliers are represented as dots. * Indicates the significant difference $p < 0.05$.

The most common third ventricle shape seen was the convex shape when comparing both the control (58%) and chronic HCP (54%) groups. The least observed shape was the concave, control group (10%) and the chronic group (2%), besides the irregularly shaped third ventricles. The shape difference between the control and chronic groups was not statistically significant, p = 0.183 (Table 4.11).

Table 4.11: Evaluating the difference in proportions of patients with different shapes of the third ventricle between the controls and chronic hydrocephalus groups.

	CON	CHCP	P value	Test
Convex *[n (%)]*	29 (58)	27 (54)	0.183	χ^2
Concave *[n (%)]*	5 (10)	1 (2)		
Straight *[n (%)]*	6 (12)	7 (14)		
Round *[n (%)]*	10 (20)	13 (26)		

Irregular *[n (%)]*	0 (0)	2 (4)

Abbreviations: CON, Controls; CHCP, Chronic Hydrocephalus; χ^2, Chi-square test.

In the acute group, the most observed shape was the round (36.96%), closely followed by the convex shape (34.78%). When comparing the difference in third ventricular shape between the chronic and acute HCP groups, there was no statistically significant difference (p = 0.303) (Table 4.12).

Table 4.12: Evaluating the difference in proportions of patients with different shapes of the third ventricle between the acute and chronic hydrocephalus groups.

	CHCP	AHCP	P value	Test
Convex *[n (%)]*	27 (54)	16 (34.78)	0.303	χ^2
Concave *[n (%)]*	1 (2)	3 (6.52)		
Straight *[n (%)]*	7 (14)	9 (19.57)		
Round *[n (%)]*	13 (26)	17 (36.96)		
Irregular *[n (%)]*	2 (4)	1 (2.17)		

Abbreviations: CHCP, Chronic Hydrocephalus; AHCP, Acute Hydrocephalus; χ^2, Chi-square test.

The graphical representations of the difference in the distribution of the third ventricular shape between the control and chronic HCP groups, as well as the chronic and acute HCP groups (Figure 4.5).

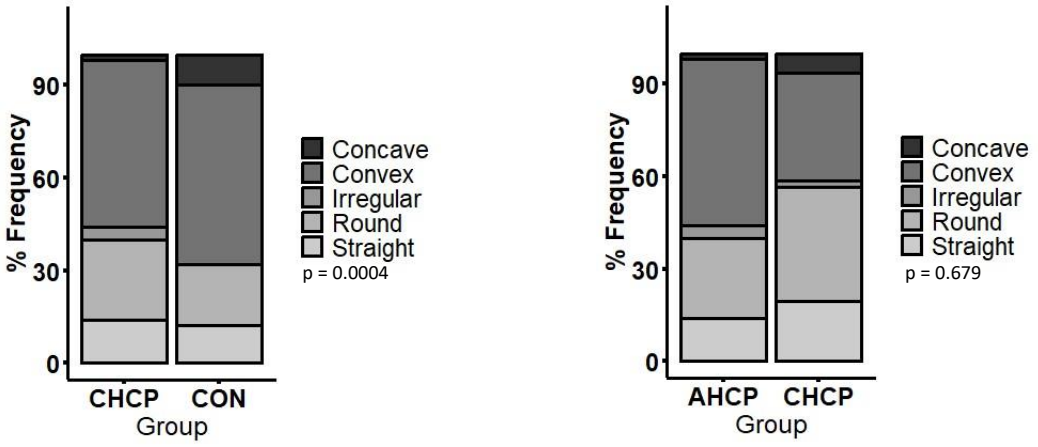

Figure 4.5: Stacked bar plot showing percentage frequencies of frontal horn shapes between controls and patients with chronic hydrocephalus on the left and patients with acute and chronic hydrocephalus on the right.

The ICC of the third ventricle were as follows: the control group had good reliability with an ICC of 0.728. The chronic and acute groups had excellent reliability with ICCs of 0.905 and 0.934, respectively.

4.2.4 Callosal Angle

The results of the CA were categorised into the angles that represented patients who had hydrocephalus (40 - 90^{o}) as well as healthy and atrophied patients (100 - 120^{o}). In the hydrocephalus category, the control group had 9 (18%), the chronic HCP group had 24 (48%) and the acute HCP group had 25 (50%). In the healthy and atrophied category, the control group had 25 (50%), the chronic HCP group had 16 (32%) and the acute HCP group had 2 (4%).

The median callosal angles in the control and chronic HCP groups were 102.30^{o} and 88.45^{o}, respectively (p = 0.01) (Table 4.13). The callosal angle difference between the acute and chronic HCP groups was not statistically different (p = 0.079) (Table 4.14).

Table 4.13: Differences in callosal angle between the control and chronic hydrocephalus groups.

	CON	CHCP	P value	Test
Angle *[median (IQR) degrees]*	102.30 (92.17 – 114.67)	88.45 (76.5 – 104.75)	0.01	MU

Abbreviations: CON, Controls; CHCP, Chronic Hydrocephalus; MU, Mann Whitney U test.

Table 4.14: Differences in callosal angle between the acute and chronic hydrocephalus groups.

	CHCP	AHCP	P value	Test
Angle *[median (IQR) degrees]*	88.45 (76.5 – 104.75)	82.40 (71.34 – 92.19)	0.079	MU

Abbreviations: CHCP, Chronic Hydrocephalus; AHCP, Acute Hydrocephalus; MU, Mann Whitney U test.

Figure 4.6 illustrates the difference in callosal angles across the groups, showing the significant difference between the control and chronic HCP groups, while there was no significant difference between the chronic and acute HCP groups.

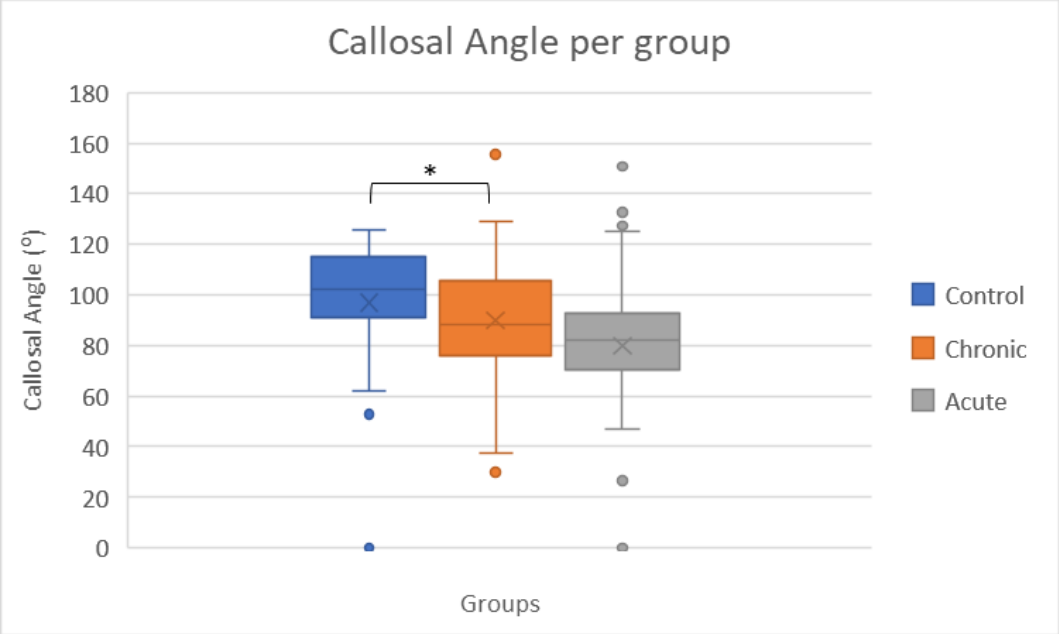

Figure 4.6: Callosal angle across the three groups. Indicating the maximum and minimum values, the first and third quartile, and the median. The mean is represented by the (x), while the outliers are represented as dots. * Indicates a significant difference $p < 0.05$.

The ICC of the callosal angles were as follows: the control group had poor reliability with an ICC of 0.241, the chronic group had excellent reliability with an ICC of 0.912 and the acute group had good reliability with an ICC of 0.829.

4.2.5 Frontal Horn Shape

This clinical feature was compared among all three groups, chronic HCP, acute HCP and the control group and this shape was described as quadrilateral or round. Tables 4.15 and 4.16 show the control group had the highest proportion of the quadrilateral shape (86%), while the acute HCP group had the highest proportion of the round shape (88%). The chronic HCP group had more scans with the quadrilateral shape (52%), than the round shape (48%).

Comparing the frontal horn shape between the control and the chronic HCP groups was statistically significant, $p = 0.02$ (Table 4.15). Similarly, comparing the frontal horn shape

between the chronic and acute HCP groups also yielded statistically significant results, p < 0.001 (Table 4.16).

Table 4.15: Evaluating the difference in proportions of the frontal horn shape between the control and chronic hydrocephalus groups.

	CHCP	CON	P value	Test
Quadrilateral *[n (%)]*	26 (52)	43 (86)	0.020	F
Round/Oval *[n (%)]*	24 (48)	7 (14)		

Abbreviations: CHCP, Chronic Hydrocephalus; CON, Controls; F, Fisher's test.

Table 4.16: Evaluating the difference in proportions of the frontal horn shape between the acute and chronic hydrocephalus groups.

	AHCP	CHCP	P value	Test
Quadrilateral *[n (%)]*	6 (12)	26 (52)	< 0.001	F
Round/Oval *[n (%)]*	44 (88)	24 (48)		

Abbreviations: AHCP, Acute Hydrocephalus; CHCP, Chronic Hydrocephalus; F, Fisher's test.

Figure 4.7 illustrates the significant difference in frequency between the chronic and acute HCP groups' frontal horn shapes.

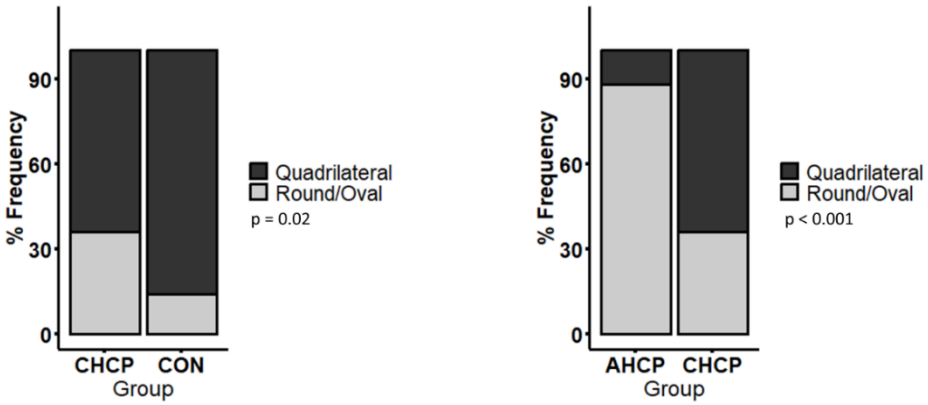

Figure 4.7: Stacked bar plot showing percentage frequencies of frontal horn shapes between the control and chronic groups on the left and between the acute and chronic hydrocephalus groups on the right.

The distribution of the ICP within the chronic and acute HCP groups is as follows; of the scans that had the quadrilateral frontal horn shape, 10 (37%) had a high ICP and 17 (63%) had a low-moderate ICP; for those that had the round/oval shape 41 (80%) had a high ICP and 10 (20%) had a low-moderate ICP. The relationship between the frontal horn shape and the intracranial pressure was evaluated using Fisher's exact test and the results were statistically significant, $p < 0.001$ (Table 4.17).

Table 4.17: Differences in proportions of frontal horn shape and its association with intracranial pressure between the chronic and acute HCP groups.

	High ICP	Low-Mod ICP	Chi-square test	Fischer's Exact test
Quadrilateral *[n (%)]*	10 (37)	17 (63)	p = 0.0002	p < 0.001 OR = 0.148
Round/Oval *[n (%)]*	41 (80)	10 (20)		

Abbreviations: ICP, Intracranial Pressure; Low-Mod, Low-Moderate; OR, Odds ratio.

4.2.6 Sylvian Fissures

The difference in width and length between the control and chronic HCP groups was statistically significant, $p < 0.001$. Additionally, within both groups, the right Sylvian fissure widths and lengths were smaller than those of the left side (Table 4.18).

Table 4.18: Differences in Sylvian fissure width and length between the control and chronic hydrocephalus groups.

	CON	CHCP	P value	Test
Width – Left *[median (IQR) mm]*	7.33 (5.65 – 8.49)	2.35 (0.00 – 5.99)	<0.001	MU
Width – Right *[median (IQR) mm]*	6.78 (5.41 – 8.30)	0.00 (0.00 – 5.31)	<0.001	MU
Length – Left *[median (IQR) mm]*	23.05 (18.48 – 27.02)	7.43 (0.00 – 22.03)	<0.001	MU
Length – Right *[median (IQR) mm]*	21.43 (16.23 – 24.80)	0.00 (0.00 – 18.9)	<0.001	MU

Abbreviations: CON, Controls; CHCP, Chronic Hydrocephalus; MU, Mann Whitney U test.

Figure 4.8 illustrates the distribution of the data and the significant difference between the lengths and widths between the control and chronic HCP groups.

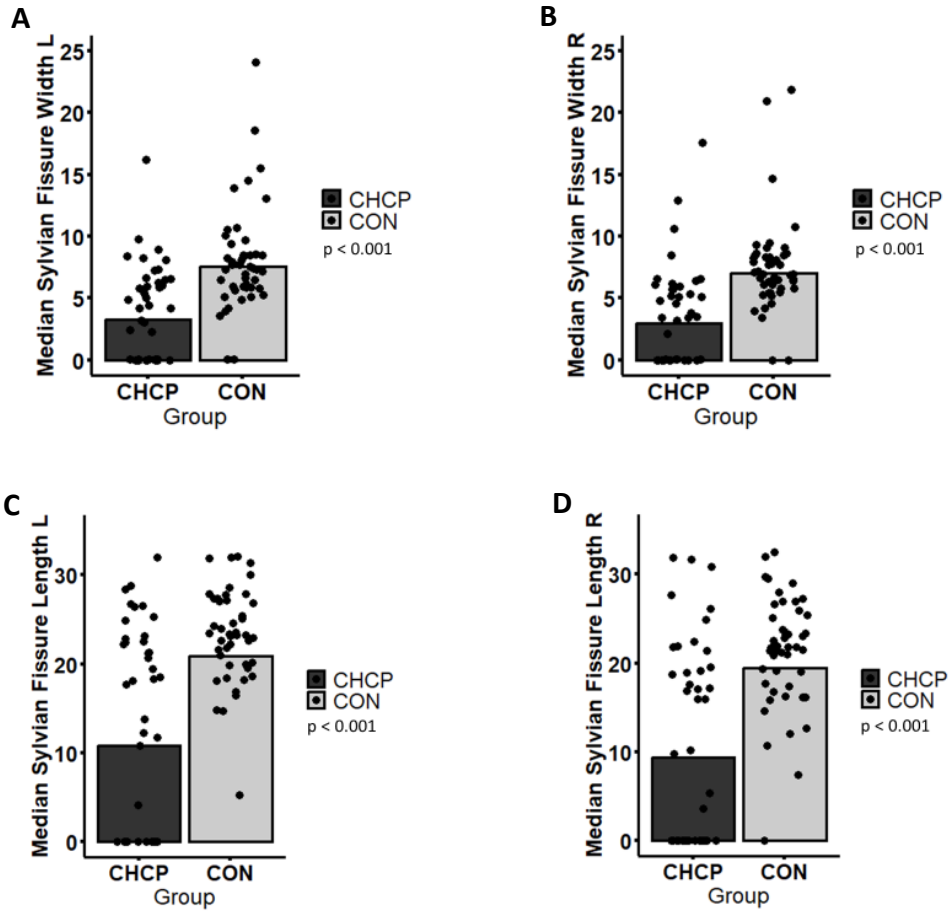

Figure 4.8: Bar plots with dots overlay showing the median distribution of Sylvian fissure measurements, respectively; A) Left side and B) Right side Sylvian fissure widths. C) Left side and D) Right side Sylvian fissure lengths. CON – control group, CHCP – chronic HCP group, L – Left, R – Right.

The difference in Sylvian fissure lengths and widths between the chronic and acute groups was not statistically significant, $p > 0.05$ (Table 4.19). Similar to the control vs chronic groups, the right side had much smaller widths and lengths than the left side, with widths as small as 0mm in both groups.

Table 4.19: Differences in Sylvian fissure width and length between the acute and chronic hydrocephalus groups.

	CHCP	AHCP	P value	Test
Width – Left *[median (IQR) mm]*	2.35 (0.00 – 5.99)	1.45 (0.00 – 3.74)	0.157	MU
Width – Right *[median (IQR) mm]*	0.00 (0.00 – 5.31)	0.00 (0.00 – 4.23)	0.605	MU
Length – Left *[median (IQR) mm]*	7.43 (0.00 – 22.03)	2.58 (0.00 – 17.33)	0.409	MU
Length – Right *[median (IQR) mm]*	0.00 (0.00 – 18.9)	0.00 (0.00 – 17.33)	0.577	MU

Abbreviations: CHCP, Chronic Hydrocephalus; AHCP, Acute Hydrocephalus; MU, Mann Whitney U test.

Figure 4.9 illustrates the chronic and acute HCP groups' loose distribution of the Sylvian fissure lengths and the tight distribution of the widths, with a difference that was not significant between them, $p > 0.05$.

The ICC results of the left Sylvian fissure lengths were as follows: the control group had poor reliability with an ICC of 0.264, the chronic group had good reliability with an ICC of 0.873 and the acute group had moderate reliability with an ICC of 0.688. The right Sylvian fissure lengths showed the following results: the control and chronic groups had good reliability with ICCs of 0.796 and 0.764, respectively. The acute group had moderate reliability with an ICC of 0.651.

The ICC results of the left Sylvian fissure widths were as follows: the control group and the chronic groups had poor reliability with ICCs of 0.262 and 0.115, respectively. The acute group had moderate reliability with an ICC of 0.652. The right Sylvian fissure width results were as follows: the control group had moderate reliability with an ICC of 0.737, the chronic group had poor reliability with an ICC of 0.142 and the acute group had good reliability with an ICC of 0.793.

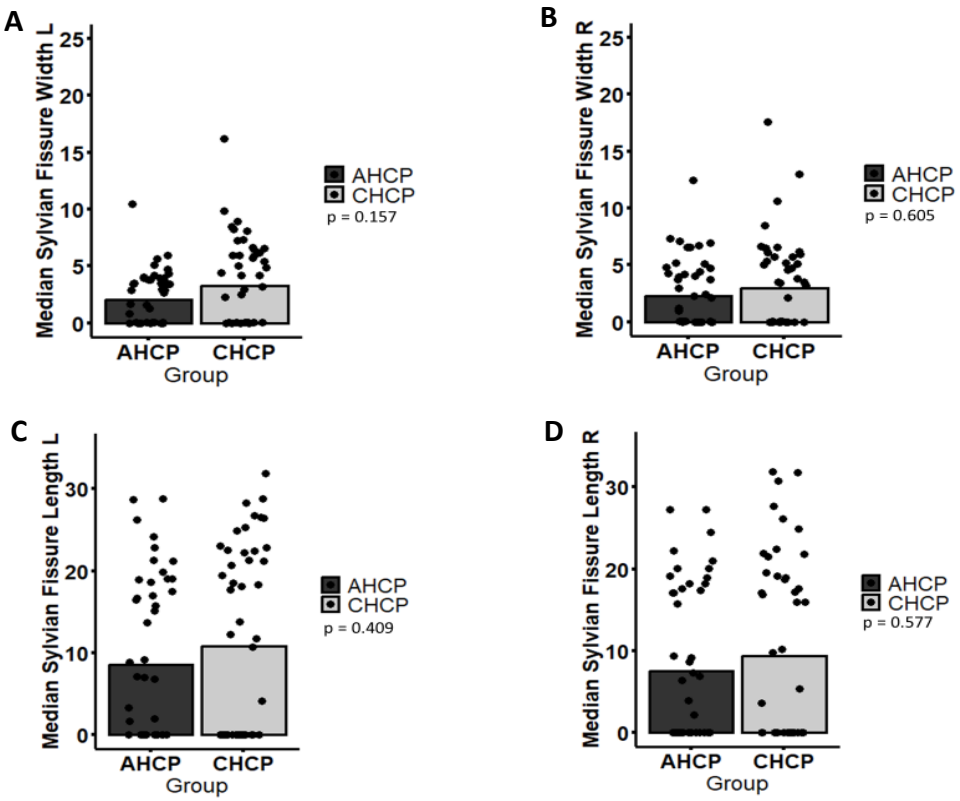

Figure 4.9: Bar plots with dots overlay showing the median distribution of Sylvian fissure measurements, respectively; A) Left side and B) Right side Sylvian fissure widths. C) Left side and D) Right side Sylvian fissure lengths. AHCP – acute HCP group, CHCP – chronic HCP group, L – Left, R – Right.

4.2.7 Periventricular White Matter Changes

All three groups, controls, chronic and acute HCP, had a large proportion of the data stating no change in PWMC, with proportions > 60% in the chronic HCP and control groups. The acute HCP group almost had an equal amount of data showing the presence of PWMC (42%) and that showing no changes (58%). Comparing the PWMC between the controls and chronic HCP groups (Table 4.20) and between the chronic and acute HCP groups (Table 4.21) yielded non-statistically significant results, with $p = 0.521$ and $p = 0.682$, respectively. The Spearman's rank correlation data for the periventricular white matter changes was negative, $p = 0.216$.

Table 4.20: Differences in proportions of the presence of periventricular white matter changes between the control and chronic HCP groups.

	CON	CHCP	P value	Test
Yes *[n (%)]*	14 (28)	18 (36)	0.521 OR = 0.694	F
No *[n (%)]*	36 (72)	32 (64)		

Abbreviations: CON, Controls; CHCP, Chronic Hydrocephalus; F, Fisher's test.

Table 4.21: Differences in proportions of the presence of periventricular white matter changes between the chronic and acute hydrocephalus groups.

	CHCP	AHCP	P value	Test
Yes *[n (%)]*	18 (36)	21 (42)	0.682 OR = 0.779	F
No *[n (%)]*	32 (64)	29 (58)		

Abbreviations: AHCP, Acute Hydrocephalus; CHCP, Chronic Hydrocephalus; F, Fisher's test.

Figure 4.10 illustrates the non-statistically significant difference in PWMC between the controls and chronic HCP groups and between the chronic and acute HCP groups.

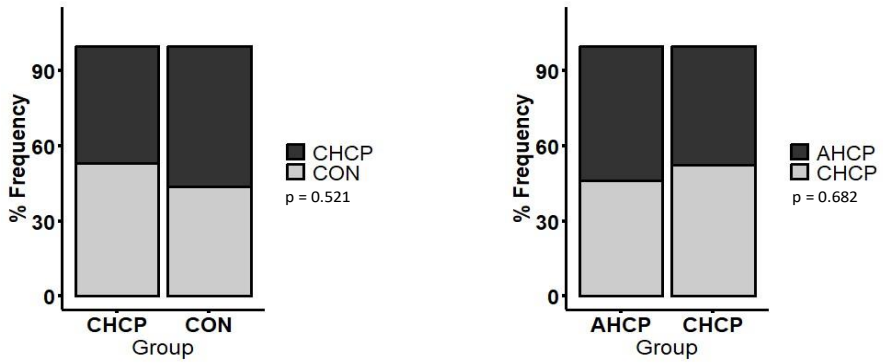

Figure 4.10: Stacked bar plot showing percentage frequencies of periventricular white matter changes between the control and chronic groups on the left and between the acute and chronic hydrocephalus groups on the right.

4.3 Summary of Results

The Evans index was significantly different between the control and chronic HCP groups ($p = 0.001$), where the chronic HCP group had a higher proportion (82%) of scans with an EI > 0.3. Between the chronic and acute HCP groups, there was no significant difference in EI ($p = 0.556$) and the proportion of scans with an EI > 0.3 was almost equal (82% and 80%, respectively).

The results for the left and right temporal horn widths indicate that they were larger in the chronic HCP group than in the control group and this difference was significant ($p = 0.003$). The acute HCP had significantly larger temporal horn widths on both the left and right sides. In all three groups, the left widths were larger than the right. Comparing the proportion of scans that had temporal horn widths > 6.0mm between the control and chronic HCP groups ($p = 0.126$ on the left and $p = 0.053$ on the right), as well as the right temporal horn widths between the chronic and acute HCP ($p = 0.171$) groups didn't yield significant results.

The control group had the smallest third ventricle widths and the acute HCP group had the largest third ventricle width. The difference in third ventricle width between the control and chronic HCP groups was significant ($p < 0.001$), this was not the case between the chronic and acute HCP groups ($p = 0.679$). The third ventricle shape that was most common in the control and chronic HCP groups was the convex shape (58% and 54%, respectively), in the acute HCP group the round shape (36.96%) was the most common.

The control group had the highest proportion (50%) of scans with CAs that were in the healthy and atrophied category. The chronic and acute HCP groups had high proportions of scans that were in the hydrocephalus category, 48% and 50%, respectively. The difference in CA

between the control and chronic HCP groups was significant ($p = 0.01$), between the chronic and acute HCP groups, it was not significant ($p = 0.079$).

The proportion of the quadrilateral frontal horn shape was high in the control (86%) and in the chronic HCP group it was 52%, the difference in proportion between the two groups was significant ($p = 0.020$). The acute HCP group had a high proportion of the round/oval shape (88%), the difference in proportion between the acute and chronic HCP group was also significant ($p < 0.001$). Comparing the relationship between the frontal horn shape and the ICP measurement, showed a high proportion (80%) of patients whose ICP was recorded as high had a round/oval shape and a high proportion (63%) of patients whose ICP was recorded as low-moderate had the quadrilateral shape. These results were significant, $p = 0.0002$.

The difference in Sylvian fissure widths and lengths between the control and chronic HCP groups was significant ($p < 0.001$). However, between the chronic and acute HCP groups, it was not ($p > 0.05$). In all three groups, the right side had smaller measurements than the left side and there was a high proportion (> 57%) of scans with no periventricular white matter changes. Comparing the difference in proportions between the control and chronic HCP groups and between the chronic and acute HCP groups yielded no significant results ($p > 0.05$).

Chapter 5: Discussion

This study describes ventricular morphometrics in chronic hydrocephalus and the potential for frontal horn shape to act as a non-invasive diagnostic marker to differentiate between acute and chronic hydrocephalus patients.

The study compared three groups: chronic HCP, acute HCP, and a control group. The acute HCP group was made up of patients who had raised ICP, while the chronic HCP group had normal or low ICP. The control group consisted of patients who had general age-related brain atrophy. The morphometrics of these three groups were compared to assess the differences between them and the relationship between the features and the clinical diagnosis.

5.2 Clinical (Radiological) features

5.2.1 Evans Index

An EI of more than 0.3 suggests ventriculomegaly, associated with hydrocephalus (Iseki *et al.*, 2009). In this study, the median EI was 0.3 (Table 4.3) for the control group, cerebral atrophy may account for this Evans index as a decrease in brain tissue results in an increased volume of CSF (Iseki *et al.*, 2009). This suggests that the patients in the control group did not have ventriculomegaly.

Similarly, Jaraj *et al.,* (2017) found that one in five people in their study had ventricular enlargement despite not having HCP. Their study looked at patients over the age of 70 years and sought to measure the EI in the normal adult population where they reported a mean EI of 0.28 (Jaraj *et al.*, 2017). While the ventricles were enlarged, the EI showed normalcy and

this enlargement was due to white matter loss. The study conducted by Jaraj *et al.,* (2017) differs from the current study in that its participants were drawn from the general community, which could account for their slightly lower EI than the EI of 0.3 reported in the current study.

In the current study, when the EI was compared between the control and chronic HCP groups, the chronic HCP group had a significantly larger EI than the control group (Figure 5.1). The chronic HCP group had larger bifrontal measurements, which suggests that the ventricles were enlarged, leading to a higher EI. This was unlike what was observed when comparing the difference in EI between the chronic and acute HCP groups. Both groups had a median EI larger than 0.3, the difference between these two groups was minor and insignificant (Table 4.4), therefore, the EI cannot be used to differentiate between the two groups, it can just be used to identify hydrocephalus.

Similar to the current study, Hashimoto *et al.,* (2010) reported a mean EI of 0.35 when they were investigating the EI in patients with idiopathic normal pressure hydrocephalus (iNPH), a type of chronic HCP. Whereas Fukuhara and Luciano (2001) reported a mean EI of 0.4 when they studied patients with late-onset idiopathic aqueduct stenosis (a type of chronic HCP). This EI (of 0.4) was seen for some individual scans in the current study, these scans could be those belonging to patients who had triventricular (non-communicating) hydrocephalus just like the patients in the study by Fukuhara and Luciano (2001).

Triventricular hydrocephalus affects the paired lateral and third ventricles, the CSF doesn't drain into the rest of the system therefore the three affected ventricles will increase in size. Whereas in communicating hydrocephalus the entire ventricular system is affected, therefore the accumulated fluid is spread within a larger space.

Unlike the two aforementioned studies that looked at two different types of HCP, the current study did not differentiate between the different types of HCP as the reporting of the condition at GSH was not specific. Nevertheless, these different types of chronic hydrocephalus all have an EI of greater than 0.3 an indicator of ventriculomegaly (Damasceno, 2015; Roblot *et al.*, 2021).

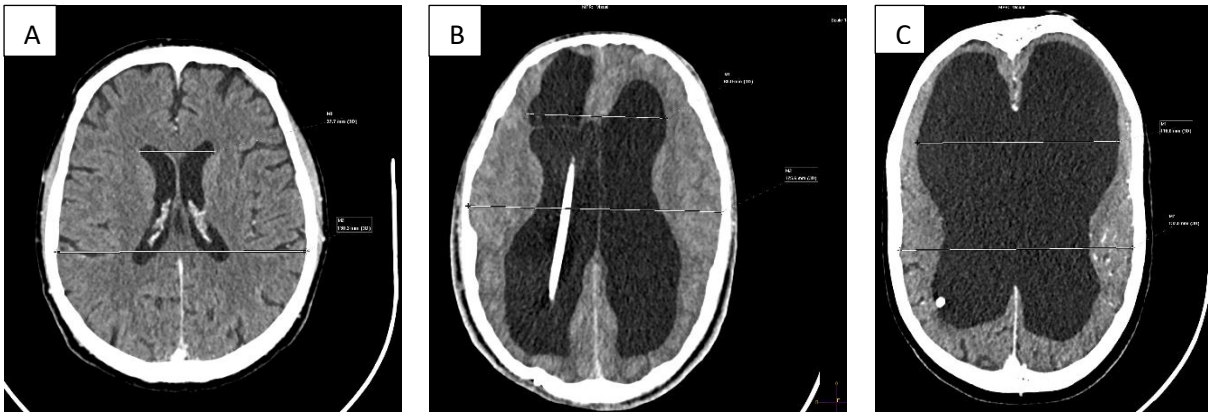

Figure 5.1: CT scans displaying the difference in the lateral ventricular size and evidence of the different Evans Indices. A) is a patient who was in the control group, B) belonged to the chronic HCP group and C) belonged in the acute HCP group.

5.2.2 Temporal Horn Width

The median temporal horn widths from the control group were smaller than those from the chronic HCP group). This does not align with Kojoukhova *et al.,* (2015) who reported a larger mean temporal horn width in the group without HCP and a smaller mean width in the group with HCP. They accounted for the larger temporal horn width in the group without HCP to the high degree of cerebral atrophy, this could mean the degree of cerebral atrophy in the control group of the current study was not high.

In this study, the right side had smaller widths than the left side in both the control and chronic HCP groups (Table 4.5). Contrary to what was observed in a study by Kojoukhova *et*

al., (2015) where they reported no significant difference in mean width between the left and right temporal horns (Kojoukhova *et al.*, 2015).

Between the chronic and acute HCP groups, the acute group had larger temporal horns on both sides. The acute HCP group having larger temporal horns is a result of having larger lateral ventricles as previously reported from the larger EI seen in the acute HCP group, which shows ventriculomegaly. Notably, there were instances where the temporal horns exhibited greater size in the chronic HCP group when compared to the acute HCP group (Figure 5.2). This variation may be influenced by the specific type of chronic HCP that a patient is experiencing.

In a study by Bao *et al.,* (2016), two investigators reported the average temporal horn width on the left and right of 8.5mm and 10.24mm, respectively, which was slightly smaller than what was reported in the current study on the left side (9.65mm) but larger than what was reported on the right side (8.48mm). In a study by Lilja-Lund *et al.,* (2020), the mean temporal horn width was 3.6mm (Lilja-Lund *et al.*, 2020), while Andersson *et al.,* (2017) and Kockum *et al.,* (2018) chose a temporal horn width limit of 4mm in their studies (Andersson *et al.*, 2017; Kockum *et al.*, 2018). All four of these studies by Bao *et al.,* (2016), Lilja-Lund *et al.,* (2020), Andersson *et al.,* (2017) and Kockum *et al.,* (2018) had participants over the age of 50 years, perhaps the age may have contributed to the smaller temporal horn widths that they reported, the relationship of temporal horn width and age was not assessed the current study.

The same trend is seen between the chronic and acute HCP groups, where the right side had temporal horn widths smaller than the left side in both groups, this data may suggest that ventricular dilation favoured the left side more than it did the right side. In contrast to the

current study, Kojoukhova *et al.,* (2015), Bao *et al.,* (2016), and Lilja-Lund *et al.,* (2020) reported an average temporal horn width on both sides rather than the temporal horn widths on both sides. They claim this is because there was no significant difference between the two sides.

The following findings from this study can be reported in relation to what is thought to be a width suggestive of HCP in the literature, this width being greater than 6.0mm (Yin *et al.,* 2021). The majority of patients in all three groups had temporal horn widths on both the left and right sides that were larger than 6.0 mm. The acute HCP group had the highest number of patients with temporal horn widths above 6.0mm, whereas the control group had the lowest proportion of such individuals. It was expected that the acute HCP group would have the highest percentage of patients with temporal horn widths more than 6.0 mm since they had the largest EI and, thus, the maximum degree of ventriculomegaly.

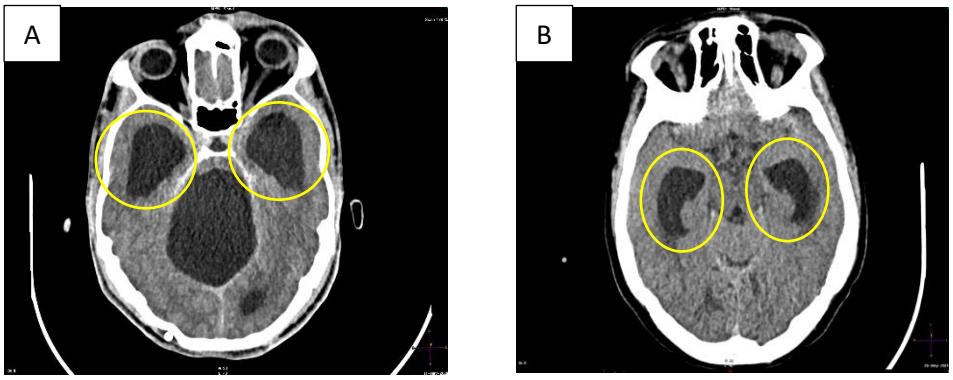

Figure 5.2: CT scans showing the temporal horns of patients with A) chronic HCP and B) acute HCP, circled in yellow.

5.2.3 Third ventricle width and shape

When the control group was compared to the chronic HCP group, the median third ventricle width was significantly reduced. There is evidence that accumulation of CSF causes ventriculomegaly, and in the case of non-communicating hydrocephalus, this would further

explain the difference in third ventricle width between the two groups (control and chronic HCP). The non-communicating or triventricular HCP types largely affect the paired lateral and the third ventricles (Bianchi *et al.*, 2021; Green *et al.*, 2021) and the fact that the excess CSF cannot be drained into the rest of the system means that those three ventricles are primarily affected. Perhaps the patients who had triventricular HCP also contributed to the third ventricle being larger in the chronic HCP group.

Fukuhara and Luciano (2001) reported a mean third ventricle width of 15.2mm in their study, about 3mm more than what was found in the current study. Perhaps it is because the patients in their study group had triventricular chronic HCP, specifically LIAS. The current study did not focus on a specific type of chronic HCP. Virhammar *et al.,* (2014) measured their clinical features in patients with iNPH and they reported a mean third ventricle width of 12mm, which is the same width reported in the current study.

When comparing the chronic and acute HCP groups, there was a small difference in median width. The widths of the chronic and acute HCP groups did not show significant differences, mirroring the lack of statistical significance in their Evans index disparity.

The current study observed the different third ventricle shapes (Figure 5.3). Whereas studies by Bao *et al.,* (2016) and Capone *et al.,* (2020), focused more on the width of the third ventricle than on the shape of the ventricle, even though it is known in the literature that there is a difference in shape (Bao *et al.*, 2016; Capone *et al.,* 2020).

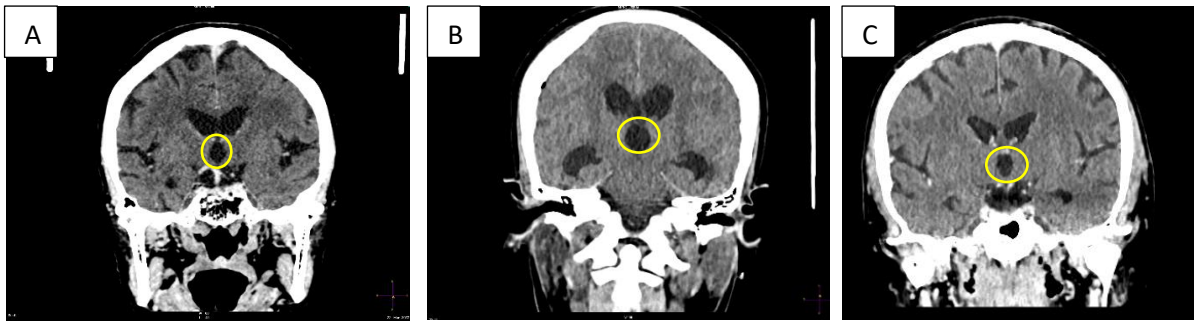

Figure 5.3: CT scans showing the different third ventricle shapes encircled in yellow, A) convex shape, B) round shape and C) straight shape.

5.2.4 Callosal angle

The results of the CA were categorised into the angles that represented patients who had hydrocephalus (40^{o} - 90^{o}) as well as healthy and atrophied patients (100^{o} - 120^{o}) (Yin *et al.,* 2021). The control group had the largest median CA (102.30^{o}) among all three groups (Figure 5.4), as anticipated given that healthy and atrophied patients typically have CAs between 100^{o} and 120^{o}. The chronic and acute HCP groups had CAs that fell within the HCP category, with median CAs of 86.92^{o} and 82.40^{o}, respectively (Figure 5.4). Similar to what was reported by Bao *et al.,* (2016), whose CA measurements were 82.97^{o} and 91.58^{o}. The CA is thought to be a ventricular-size marker (Kojoukhova *et al.*, 2015), and the acute group in this study had the lowest angle, which represents the degree of lateral ventricular dilatation.

Comparing the difference in CAs between the control and chronic groups was significant. This was a comparison between two groups that fell within two different categories, the HCP, and the healthy and atrophied categories, respectively. On the other hand, the difference between the chronic and acute HCP groups was not significant. Both these groups fell within the HCP group, with angles that were close in size.

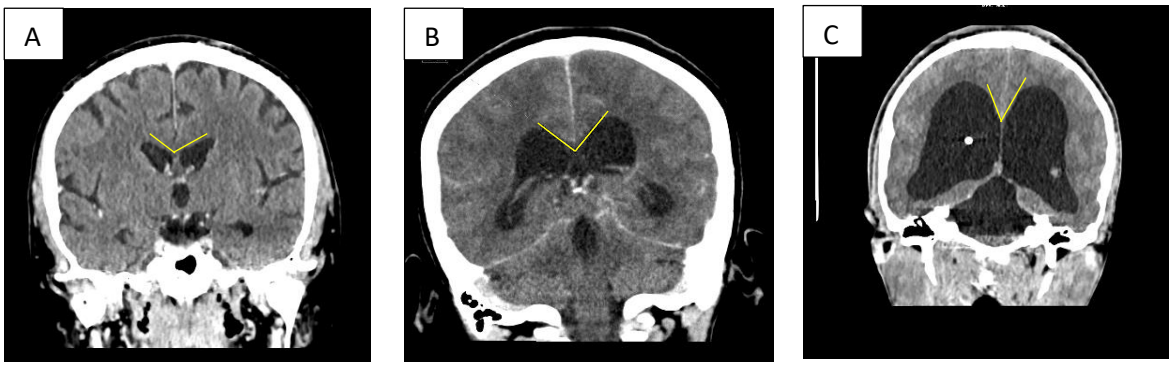

Figure 5.4: CT scans showing the callosal angles of patients in the A) control group, B) chronic HCP and C) acute HCP group.

5.2.5 Frontal horn shape and Intracranial pressure

This study aimed to characterize the observed shape of the frontal horns and evaluate the variation in frontal horn shape among the three groups: the control, chronic, and acute HCP groups. This feature is unique and has not been previously described in the literature. The two shapes identified were the quadrilateral shape, with an obtuse angle in between the horns and the round shape which has an acute angle in between, both observed in the axial plane (Figure 5.5).

The chronic HCP group had a proportion of 52%, while the control group had a higher percentage of scans (86%) with the quadrilateral shape. However, the majority of scans (88%) in the acute group exhibited a round shape linked to the acute angle between the frontal horns; this finding could have been brought on by a build-up of CSF. Cerebrospinal fluid storage is correlated with the ventricles' conformity (Filis *et al.,* 2017), perhaps the change in frontal horn shape occurs once the ventricles are not able to conform to the increased volume of CSF.

Cerebrospinal fluid volume affects ICP, a known indicator of HCP (Evensen and Eide, 2020). Furthermore, Rangel-Castillo *et al.,* (2008) stated that the measurement of ICP indicates the

severity of the condition; from chronic, to acute and severe. However, as mentioned previously, measuring the ICP is an invasive procedure and in trying to find an alternative, non-invasive manner of diagnosis, assessing the relationship between the frontal horn shape and the ICP was the focus of this study.

The scans that showed the quadrilateral frontal horn shape belonged to 63% of scans that were from patients whom the surgeon reported to have a low-moderate ICP. While 80% of the scans that showed the round/oval shape were those that belonged to patients who were reported to have a high ICP, measured during surgery. This assessment yielded significant results.

This unique feature could be used when diagnosing patients suspected of having hydrocephalus and differentiate between those who may have acute hydrocephalus and those who may have chronic hydrocephalus. This study suggests that it is likely that this feature may aid in the differentiation of patients with acute hydrocephalus and those with chronic hydrocephalus, during diagnosis.

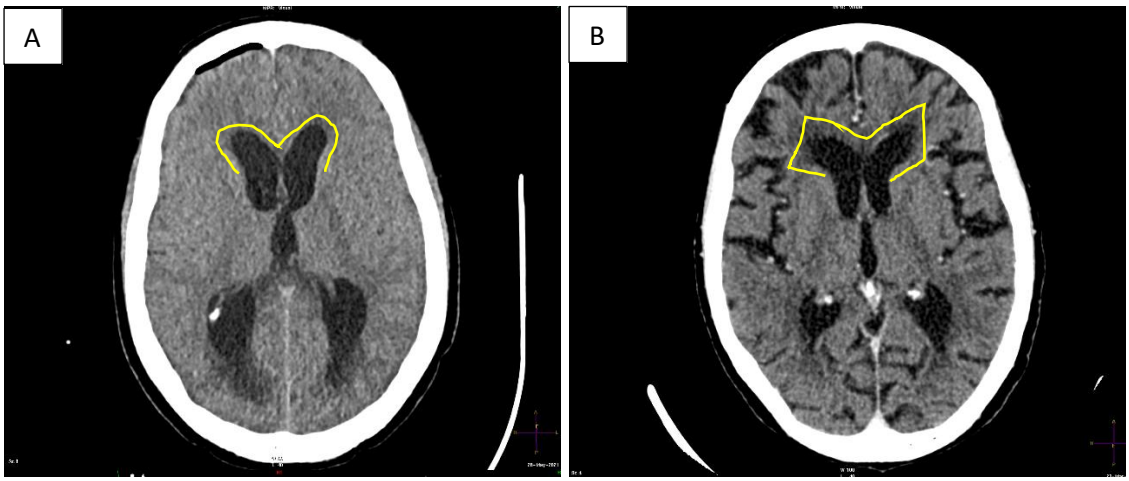

Figure 5.5: CT scans showing the A) round and B) quadrilateral frontal horn shapes.

5.2.6 Sylvian Fissures

Hashimoto *et al.,* (2010) reported the Sylvian fissures to be 'dilated' in 96% of their chronic HCP sample, however, their observation was not quantitative as opposed to the current study where measurements of the Sylvian fissures were taken. Comparably Johannsson *et al.,* (2022) described the appearance of the fissures subjectively as 'dilated' in 79.3% of their sample, unlike in the current study, where the Sylvian fissure heights and widths were observed and measured.

The control group in the current study had Sylvian fissures that were more dilated than those in the chronic HCP group, which opposes what was reported in the studies by Hashimoto *et al.,* (2010) and Johannsson *et al.,* (2022) where the Sylvian fissures were more dilated in the hydrocephalus group. The excess CSF in the control group was stored in the Sylvian fissures, whereas in the chronic HCP group, it may have been stored in the ventricles. The difference in size between the control and chronic HCP groups was significant. Similar to the temporal horns, the widths and lengths of the Sylvian fissures were smaller on the right compared to the left.

The chronic and acute HCP groups did not have any significant differences. All measurements had a minimum of 0.0mm in both groups (Figure 5.6), this therefore opposes the findings by Nakajima *et al.,* (2021) which state that the Sylvian fissure dilation is an indicator of the dysfunction in CSF dynamics (Nakajima *et al.*, 2021). Furthermore, the right side had smaller sizes compared to the left. Virhammar *et al.,* (2014) reported a mean Sylvian fissure height of 6mm in their study of iNPH patients, which was different to what was found in the current study, where the median Sylvian fissure heights were less than 4mm. The excess CSF was stored in the ventricles rather than in the Sylvian fissures.

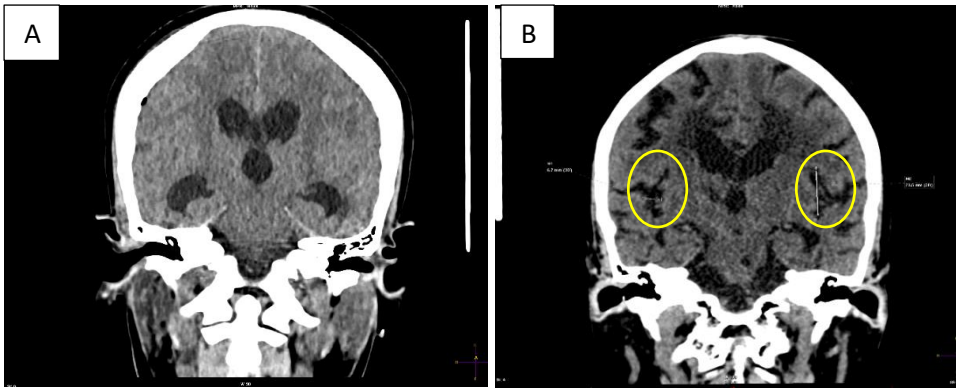

Figure 5.6: CT scans showing the Sylvian fissures. A) shows compressed Sylvian fissures, while B) shows dilated Sylvian fissures.

5.2.7 Periventricular white matter changes

The control group had the highest proportion of scans that did not show PWMC, which is anticipated as there is no excess fluid build-up and the pressure in the lateral ventricles is normal. The control group had the smallest proportion (28%) of scans that showed PWMC, while the acute HCP group had the highest proportion (42%) of scans that showed periventricular white matter changes. In a study by Hashimoto *et al.,* (2010), they reported that 52% of their study population had mild or moderate white matter changes and 14% of their study population had severe white matter changes. The PWMC findings of the current study, as well as the study by Hashimoto *et al.,* (2010), suggest that there was insufficient pressure within the ventricles to cause excessive fluid to leak into the brain parenchyma.

The increased accumulation of CSF and the raised pressure that causes the CSF to infiltrate past the ependymal cell layer enclosing the lateral ventricles and into the brain parenchyma could be the reason the acute group would have the largest proportion (Casaca-Carreira *et al.*, 2018). This change presents as white patches around the lateral ventricles, as shown by the arrows in Figure 5.7.

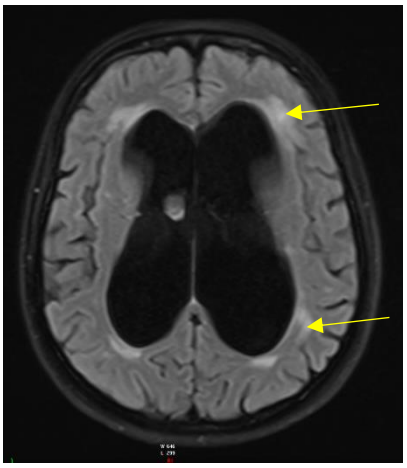

Figure 5.7: An MRI scan showing the periventricular white matter changes around the lateral ventricles, indicated by the yellow arrows.

5.3 Conclusion

In conclusion, when comparing the clinical features between the chronic HCP and control groups, it was evident that the features were much larger in the chronic HCP group, as a result of the accumulation of CSF. When comparing the chronic and acute HCP groups, the ventricles, and the temporal horns, were larger in the acute HCP group as a result of the degree of ventriculomegaly. Conversely, the Sylvian fissures and the CA were smaller in the acute HCP group.

As the literature suggests, the ventricles become so enlarged that the CA becomes smaller to accommodate the increase in CSF volume. What was different from the literature was the lack of dilation of the sylvian fissures in this study which would make sense in the case of patients who had non-communicating HCP, as CSF accumulates in the paired lateral and third ventricles. In the communicating HCP cases, however, it might have been because the CSF accumulated mostly in the ventricles. The data also revealed that the right side had smaller measurements compared to the left side, which may suggest that ventricular and CSF space dilation favoured the left side more than it did the right side.

The frontal horn shape is a unique and unstudied feature that requires more research to be done. When closely examined, one can discern a subtle variation in the shape of the frontal horns, some of which may be more noticeable than others. There is potential in using the frontal horn shape as a non-invasive diagnostic marker for differentiating between chronic and acute hydrocephalus in the clinical space.

When it came to the more subjective evaluations, interobserver agreement was lower than it was for the quantitative measurements. The researchers who study hydrocephalus record the largest or widest measurements with not much of an explanation as to how to do so. The only

clinical feature that is well explained in terms of exactly how it is measured is the CA, it has precise reference points. In the current study, the researcher and the inter-observer took multiple measures and recorded the largest or widest measurement to mitigate this issue of uncertainty.

The issue of reliability highlights the necessity for standardised evaluations and objective measurements. The clinical heterogeneity of hydrocephalus among patients continues to be a challenge in the research of the condition (Hochstetler *et al.,* 2022).

5.4 Study limitations and recommendations

Limitations

1. General to hydrocephalus studies is the fact that with some of the measurements, there is insufficient information regarding reference points that measurements are taken from. The only measurement that has specifics on how to take the measurement is the callosal angle.
2. The current study used patients who had generalised cerebral atrophy as controls, as opposed to healthy individuals.
3. The periventricular white matter changes would have been better assessed using MRI scans instead of CT scans, to see the changes.
4. The subjective nature of purposive sampling may have resulted in sample selection bias.
5. Third ventricle shape comparison could not be made as the studies in the literature focused more on the metrics than the shape of the ventricle.

Recommendations

1. It is recommended that in future research, healthy individuals be included as controls to reduce the potential for confounding effects from other brain diseases.
2. Clarity on important reference points, so that other researchers may be able to reproduce the research with ease.

Chapter 6: Conclusion

This observational study aimed to assess the clinical features observed on scans of patients diagnosed with HCP. The current study examined patients who were diagnosed with HCP, acute and chronic, as well as a control group. The morphometric data of seven clinical features was observed and recorded. This data was then compared among the groups to assess the differences between the groups. Additionally, this data was examined to see if there was a relationship between the data and the diagnosis of the condition, whether acute or chronic. The data obtained from the current study was compared to existing published studies.

The clinical features that were examined were those commonly observed on the MRI or CT scans of patients with HCP, all the clinical features have been described in the literature except the frontal horn shape. Furthermore, in the South African context, this data is not sufficient. Therefore, the purpose of this study was to measure the morphometrics and to further describe the unique frontal horn shape that was observed on the MRI and CT scans of patients with HCP in addition to the ones previously described. These features have not been described within the South African context. The features will be explained in the subsequent paragraphs.

The first was the Evans index, the current study's findings were consistent with the literature. The control group had an Evans index of 0.3, which borders what would be considered ventricular enlargement. This index was perhaps a result of the control group comprising patients with generalised cerebral atrophy, who would generally have a build-up of CSF to compensate for the lost brain matter. The chronic and acute HCP groups had an EI considered

hydrocephalic, and the acute HCP group had a slightly larger EI, indicating the degree of ventriculomegaly.

The temporal horns were the largest in the acute group, and as the temporal horns are a part of the ventricular system, the more fluid retained in the ventricles the larger the parts of the ventricles will be. Just like the EI was influenced by the degree of ventriculomegaly, so were the temporal horns. Therefore, the trend seen in the EI observation was also seen with the temporal horn widths.

The current study's temporal horn data was in keeping with the literature, the only aspect not reported was the side that was most affected by the condition. In the current study the right side had smaller temporal horns, most studies calculated an average of both sides and reported that mean value. Even so, the measurements were close to what was reported by other researchers.

The median third ventricle widths reported in this study were +/- 2mm larger than the widths reported in the literature. One explanation could be that in most of the studies in the literature, the researchers focused on a specific type of chronic hydrocephalus, whereas this study did not. The ventricles in communicating and non-communicating hydrocephalus' become enlarged in different ways. The non-communicating hydrocephalus', because it only affects the paired lateral and third ventricles would be the areas that would be more dilated. As opposed to communicating hydrocephalus' which would allow for the fluid to be distributed within the ventricular system and the CSF spaces in the brain.

Therefore, had this study focused on a specific type of chronic hydrocephalus like the other studies, the results would probably have been closer to what has been reported in the

literature. Nonetheless, the widths reported were still indicative of ventricular enlargement and thus HCP.

The shape of the third ventricle was well explained in this study and the most common shape observed was the concave shape, consistent with what has been described in review studies. It was uncommon to find a population study that reported on third ventricle shape, however, it is still considered a contributing radiological marker for diagnosing hydrocephalus.

The CAs reported were in keeping with the literature. The control group had a median CA that fell into the healthy and atrophied category, where the angles measured ranged between 100^{o} and 120^{o}. The chronic and acute groups had median CAs that also followed what was in the literature, the measured angles ranged between 40^{o} - 90^{o}. This angle is one of the most well-explained clinical features of HCP, even the positioning of the scan is very specific to get the correct position for measuring. It was one of the easiest measurements to take and reproduce.

The frontal horn shape is a unique feature observed on the MRI and CT scans. The description of this shape sought to differentiate between patients with acute and chronic HCP. This was done in conjunction with the ICP reported by the surgeons, just to assess the relationship between the ICP and the diagnosis of HCP.

In the current study, the round shape was observed on scans of patients who were reported to have acute HCP and the ICP reading for most of these scans was high. The quadrilateral shape observed on the scans mostly had a moderate or low ICP reading. This is an indication that the frontal horn shape may be used as a non-invasive diagnostic marker during patient examination, to differentiate between acute and chronic HCP patients. Particularly because acute HCP patients require urgent care to avoid further brain matter damage.

The Sylvian fissures in this study showed results that were not consistent with the literature. It is clear from the literature that the Sylvian fissures of most patients who have HCP should be dilated, due to fluid accumulation. This was not the case in this study, perhaps some ventricles were so enlarged that the fissures could not accumulate much fluid and they then remained narrow or compressed.

The acute HCP group, which would be expected to have the highest volume of CSF due to the EI reported, had the highest proportion of scans with PWMC. This fluid buildup becomes so much that the fluid seeps into the adjacent brain tissue. The only recommendation here would be that these changes be examined on MRI scans rather than CT, as they are much easier to see on an MRI scan.

This study aimed to examine clinical features that are associated with HCP and to not only add to the literature globally but to address the condition in the adult South African population. The clinical features, for the most part, were consistent with the literature, however, some deviated a bit from the literature. The only feature not described in the literature, the frontal horn shape, holds potential in the clinical space and should further be researched and trialled to see if it can be successfully used in diagnosing HCP and differentiating between chronic and acute HCP.

References

Adigun, O.O. and Al-Dhahir, M.A. (2021) 'Anatomy, Head and Neck, Cerebrospinal Fluid', in *StatPearls*. Treasure Island (FL): StatPearls Publishing. Available at: http://www.ncbi.nlm.nih.gov/books/NBK459286/ (Accessed: 25 August 2021).

Agarwal, A., Bathla, G. and Kanekar, S. (2016) 'Imaging of Communicating Hydrocephalus', *Seminars in Ultrasound, CT and MRI*, 37(2), pp. 100–108. Available at: https://doi.org/10.1053/j.sult.2016.02.007.

Al-Jumaily, M. *et al.* (2012) 'Long term neuropsychological outcome and management of "decompensated" longstanding overt ventriculomegaly in adults', *British Journal of Neurosurgery*, 26(5), pp. 717–721. Available at: https://doi.org/10.3109/02688697.2012.673647.

Alvi, M.A. *et al.* (2020) 'Predictors of adverse outcomes and cost after surgical management for idiopathic normal pressure hydrocephalus: Analyses from a national database', *Clinical Neurology and Neurosurgery*, 197, p. 106178. Available at: https://doi.org/10.1016/j.clineuro.2020.106178.

Andersson, J. *et al.* (2017) 'Challenges in diagnosing normal pressure hydrocephalus: Evaluation of the diagnostic guidelines', *eNeurologicalSci*, 7, pp. 27–31. Available at: https://doi.org/10.1016/j.ensci.2017.04.002.

Andersson, J. *et al.* (2019) 'Prevalence of idiopathic normal pressure hydrocephalus: A prospective, population-based study', *PloS One*, 14(5), p. e0217705. Available at: https://doi.org/10.1371/journal.pone.0217705.

Bao, J. *et al.* (2016) 'Feasibility of Simple Linear Measurements to Determine Ventricular Enlargement in Patients With Idiopathic Normal Pressure Hydrocephalus', *Journal of Craniofacial Surgery*, 27(5), p. e462. Available at: https://doi.org/10.1097/SCS.0000000000002779.

Bianchi, F. *et al.* (2021) 'Long-standing Overt Ventriculomegaly in Adults and Endoscopic Third Ventriculostomy, the Perfect Treatment for the Proper Diagnosis', *World Neurosurgery*, 149, pp. 104–110. Available at: https://doi.org/10.1016/j.wneu.2021.02.016.

Biga, L.M. *et al.* (2019) '14.2 Blood Flow the meninges and Cerebrospinal Fluid Production and Circulation', in *Anatomy & Physiology*. OpenStax/Oregon State University. Available at: https://open.oregonstate.education/aandp/chapter/14-2-blood-flow-the-meninges-and-cerebrospinal-fluid-production-and-circulation/ (Accessed: 1 May 2021).

Bir, S.C. *et al.* (2016) 'Epidemiology of adult-onset hydrocephalus: institutional experience with 2001 patients', *Neurosurgical Focus*, 41(3), p. E5. Available at: https://doi.org/10.3171/2016.7.FOCUS16188.

Bratton, S.L. *et al.* (2007) 'VI. Indications for Intracranial Pressure Monitoring', *Journal of Neurotrauma*, 24(supplement 1), p. S-37. Available at: https://doi.org/10.1089/neu.2007.9990.

Burtscher, J. *et al.* (2003) 'Effect of endoscopic third ventriculostomy on neuropsychological outcome in late onset idiopathic aqueduct stenosis: a prospective study', *Journal of Neurology, Neurosurgery, and Psychiatry*, 74(2), pp. 222–225. Available at: https://doi.org/10.1136/jnnp.74.2.222.

Capone, P.M., Bertelson, J.A. and Ajtai, B. (2020) 'Neuroimaging of Normal Pressure Hydrocephalus and Hydrocephalus', *Neurologic Clinics*, 38(1), pp. 171–183. Available at: https://doi.org/10.1016/j.ncl.2019.09.003.

Casaca-Carreira, J. *et al.* (2018) 'Transependymal Cerebrospinal Fluid Flow: Opportunity for Drug Delivery?', *Molecular Neurobiology*, 55(4), pp. 2780–2788. Available at: https://doi.org/10.1007/s12035-017-0501-y.

Damasceno, B.P. (2015) 'Neuroimaging in normal pressure hydrocephalus', *Dementia e Neuropsychologia*, 9(4), pp. 350–355. Available at: https://doi.org/10.1590/1980-57642015DN94000350.

De Onis, M. *et al.* (2006) 'Comparison of the World Health Organization (WHO) Child Growth Standards and the National Center for Health Statistics/WHO international growth reference: implications for child health programmes', *Public Health Nutrition*, 9(7), pp. 942–947. Available at: https://doi.org/10.1017/PHN20062005.

Dewan, M.C. *et al.* (2018) 'Global hydrocephalus epidemiology and incidence: systematic review and meta-analysis', *Journal of Neurosurgery*, 130(4), pp. 1065–1079. Available at: https://doi.org/10.3171/2017.10.JNS17439.

Edwards, R.J. *et al.* (2004) 'Chronic hydrocephalus in adults', *Brain Pathology (Zurich, Switzerland)*, 14(3), pp. 325–336. Available at: https://doi.org/10.1111/j.1750-3639.2004.tb00072.x.

Edwards, R.J., Britz, G.W. and Marsh, H. (2003) 'Chronic headaches due to occult hydrocephalus', *Journal of the Royal Society of Medicine*, 96(2), pp. 77–78. Available at: https://doi.org/10.1258/jrsm.96.2.77.

Engel, D.C. *et al.* (2021) 'Incidental findings of typical iNPH imaging signs in asymptomatic subjects with subclinical cognitive decline', *Fluids and barriers of the CNS*, 18(1), p. 37. Available at: https://doi.org/10.1186/s12987-021-00268-x.

Evensen, K.B. and Eide, P.K. (2020) 'Measuring intracranial pressure by invasive, less invasive or non-invasive means: limitations and avenues for improvement', *Fluids and Barriers of the CNS*, 17, p. 34. Available at: https://doi.org/10.1186/s12987-020-00195-3.

Farb, R. and Rovira, À. (2020) 'Hydrocephalus and CSF Disorders', in J. Hodler, R.A. Kubik-Huch, and G.K. von Schulthess (eds) *Diseases of the Brain, Head and Neck, Spine 2020–2023:*

Diagnostic Imaging. Cham (CH): Springer (IDKD Springer Series). Available at: http://www.ncbi.nlm.nih.gov/books/NBK554339/ (Accessed: 25 August 2021).

Filis, A.K., Aghayev, K. and Vrionis, F.D. (2017) 'Cerebrospinal Fluid and Hydrocephalus: Physiology, Diagnosis, and Treatment', *Cancer Control*, 24(1), pp. 6–8. Available at: https://doi.org/10.1177/107327481702400102.

Fukuhara, T. and Luciano, M.G. (2001) 'Clinical features of late-onset idiopathic aqueductal stenosis', *Surgical Neurology*, 55(3), pp. 132–136. Available at: https://doi.org/10.1016/S0090-3019(01)00359-7.

Green, L.M. *et al.* (2021) 'Intracranial pressure waveform characteristics in idiopathic normal pressure hydrocephalus and late-onset idiopathic aqueductal stenosis', *Fluids and barriers of the CNS*, 18(1), p. 25. Available at: https://doi.org/10.1186/s12987-021-00259-y.

Greitz, D. (2004) 'Radiological assessment of hydrocephalus: new theories and implications for therapy', *Neurosurgical Review*, 27(3), pp. 145–165; discussion 166-167. Available at: https://doi.org/10.1007/s10143-004-0326-9.

Hakim, S. and Adams, R.D. (1965) 'The special clinical problem of symptomatic hydrocephalus with normal cerebrospinal fluid pressure. Observations on cerebrospinal fluid hydrodynamics', *Journal of the Neurological Sciences*, 2(4), pp. 307–327. Available at: https://doi.org/10.1016/0022-510x(65)90016-x.

He, W.-J. *et al.* (2020) 'Idiopathic Normal Pressure Hydrocephalus and Elderly Acquired Hydrocephalus: Evaluation With Cerebrospinal Fluid Flow and Ventricular Volume Parameters', *Frontiers in Aging Neuroscience*, 12, p. 584842. Available at: https://doi.org/10.3389/fnagi.2020.584842.

Hong, J. *et al.* (2016) 'Surgical management of arrested hydrocephalus: Case report, literature review, and 18-month follow-up', *Clinical Neurology and Neurosurgery*, 151, pp. 79–85. Available at: https://doi.org/10.1016/j.clineuro.2016.10.017.

Ibáñez-Botella, G. *et al.* (2017) 'LOVA: the role of endoscopic third ventriculostomy and a new proposal for diagnostic criteria', *Neurosurgical Review*, 40(4), pp. 605–611. Available at: https://doi.org/10.1007/s10143-017-0813-4.

Iseki, C. *et al.* (2009) 'Asymptomatic ventriculomegaly with features of idiopathic normal pressure hydrocephalus on MRI (AVIM) in the elderly: a prospective study in a Japanese population', *Journal of the Neurological Sciences*, 277(1–2), pp. 54–57. Available at: https://doi.org/10.1016/j.jns.2008.10.004.

Jaraj, D. *et al.* (2017) 'Estimated ventricle size using Evans index: reference values from a population-based sample', *European Journal of Neurology*, 24(3), pp. 468–474. Available at: https://doi.org/10.1111/ene.13226.

Kahle, K.T. *et al.* (2016) 'Hydrocephalus in children', *The Lancet*, 387(10020), pp. 788–799. Available at: https://doi.org/10.1016/S0140-6736(15)60694-8.

Kartal, M.G. and Algin, O. (2014) 'Evaluation of hydrocephalus and other cerebrospinal fluid disorders with MRI: An update', *Insights into Imaging*, 5(4), pp. 531–541. Available at: https://doi.org/10.1007/s13244-014-0333-5.

Kitagaki, H. *et al.* (1998) 'CSF spaces in idiopathic normal pressure hydrocephalus: morphology and volumetry', *AJNR. American journal of neuroradiology*, 19(7), pp. 1277–1284.

Kockum, K. *et al.* (2018a) 'The idiopathic normal-pressure hydrocephalus Radscale: a radiological scale for structured evaluation', *European Journal of Neurology*, 25(3), pp. 569–576. Available at: https://doi.org/10.1111/ene.13555.

Kockum, K. *et al.* (2018b) 'The idiopathic normal-pressure hydrocephalus Radscale: a radiological scale for structured evaluation', *European Journal of Neurology*, 25(3), pp. 569–576. Available at: https://doi.org/10.1111/ene.13555.

Kockum, K. *et al.* (2019) 'Standardized image evaluation in patients with idiopathic normal pressure hydrocephalus: consistency and reproducibility', *Neuroradiology*, 61(12), pp. 1397–1406. Available at: https://doi.org/10.1007/s00234-019-02273-2.

Kojoukhova, M. *et al.* (2015) 'Feasibility of radiological markers in idiopathic normal pressure hydrocephalus', *Acta Neurochirurgica*, 157(10), pp. 1709–1719. Available at: https://doi.org/10.1007/s00701-015-2503-8.

Leinonen, V., Vanninen, R. and Rauramaa, T. (2018) 'Chapter 5 - Cerebrospinal fluid circulation and hydrocephalus', in G.G. Kovacs and I. Alafuzoff (eds) *Handbook of Clinical Neurology*. Elsevier (Neuropathology), pp. 39–50. Available at: https://doi.org/10.1016/B978-0-12-802395-2.00005-5.

Lilja-Lund, O. *et al.* (2020) 'Wide temporal horns are associated with cognitive dysfunction, as well as impaired gait and incontinence', *Scientific Reports*, 10, p. 18203. Available at: https://doi.org/10.1038/s41598-020-75381-2.

Locatelli, M. *et al.* (2014) 'Third Ventriculostomy in Late-onset Idiopathic Aqueductal Stenosis Treatment: A Focus on Clinical Presentation and Radiological Diagnosis', *Neurologia Medico-Chirurgica*, 54(12), pp. 1014–1021. Available at: https://doi.org/10.2176/nmc.oa.2013-0367.

McAllister, J.P. (2012) 'Pathophysiology of congenital and neonatal hydrocephalus', *Seminars in Fetal and Neonatal Medicine*, 17(5), pp. 285–294. Available at: https://doi.org/10.1016/j.siny.2012.06.004.

McHugh, M.L. (2013) 'The Chi-square test of independence', *Biochemia Medica*, 23(2), pp. 143–149. Available at: https://doi.org/10.11613/BM.2013.018.

Mortazavi, M.M. *et al.* (2014a) 'The ventricular system of the brain: a comprehensive review of its history, anatomy, histology, embryology, and surgical considerations', *Child's Nervous System*, 30(1), pp. 19–35. Available at: https://doi.org/10.1007/s00381-013-2321-3.

Mortazavi, M.M. *et al.* (2014b) 'The ventricular system of the brain: a comprehensive review of its history, anatomy, histology, embryology, and surgical considerations', *Child's Nervous*

System: ChNS: Official Journal of the International Society for Pediatric Neurosurgery, 30(1), pp. 19–35. Available at: https://doi.org/10.1007/s00381-013-2321-3.

Nakajima, M. *et al.* (2021) 'Guidelines for Management of Idiopathic Normal Pressure Hydrocephalus (Third Edition): Endorsed by the Japanese Society of Normal Pressure Hydrocephalus', *Neurologia Medico-Chirurgica*, 61(2), pp. 63–97. Available at: https://doi.org/10.2176/nmc.st.2020-0292.

Oi, S. *et al.* (2000) 'Pathophysiology of long-standing overt ventriculomegaly in adults', *Journal of Neurosurgery*, 92(6), pp. 933–940. Available at: https://doi.org/10.3171/jns.2000.92.6.0933.

Oi, S. and Di Rocco, C. (2006) 'Proposal of "evolution theory in cerebrospinal fluid dynamics" and minor pathway hydrocephalus in developing immature brain', *Child's Nervous System*, 22(7), pp. 662–669. Available at: https://doi.org/10.1007/s00381-005-0020-4.

Panigrahi, M.K. *et al.* (2021) 'Diagnostic Nuances and Surgical Management of Arrested Hydrocephalus', *Neurology India*, 69(Supplement), pp. S336–S341. Available at: https://doi.org/10.4103/0028-3886.332262.

Pisapia, J.M. *et al.* (2017) 'Fetal ventriculomegaly: Diagnosis, treatment, and future directions', *Child's Nervous System: ChNS: Official Journal of the International Society for Pediatric Neurosurgery*, 33(7), pp. 1113–1123. Available at: https://doi.org/10.1007/s00381-017-3441-y.

Protection of Personal Information Act (POPI Act) (no date) *POPIA*. Available at: https://popia.co.za/ (Accessed: 16 May 2021).

Rangel-Castillo, L., Gopinath, S. and Robertson, C.S. (2008) 'Management of Intracranial Hypertension', *Neurologic clinics*, 26(2), pp. 521–541. Available at: https://doi.org/10.1016/j.ncl.2008.02.003.

Roblot, P. *et al.* (2021) 'Communicating chronic hydrocephalus: A review', *La Revue De Medecine Interne*, 42(11), pp. 781–788. Available at: https://doi.org/10.1016/j.revmed.2021.05.018.

Scelsi, C.L. *et al.* (2020) 'The Lateral Ventricles: A Detailed Review of Anatomy, Development, and Anatomic Variations', *American Journal of Neuroradiology*, 41(4), pp. 566–572. Available at: https://doi.org/10.3174/ajnr.A6456.

Shen, X.Q. *et al.* (2006) 'Expression of the water-channel protein aquaporin 4 in the H-Tx rat: possible compensatory role in spontaneously arrested hydrocephalus', *Journal of Neurosurgery: Pediatrics*, 105(6), pp. 459–464. Available at: https://doi.org/10.3171/ped.2006.105.6.459.

Stratchko, L. *et al.* (2016) 'The Ventricular System of the Brain: Anatomy and Normal Variations', *Seminars in Ultrasound, CT and MRI*, 37(2), pp. 72–83. Available at: https://doi.org/10.1053/j.sult.2016.01.004.

Tuniz, F. *et al.* (2021) 'Long-Standing Overt Ventriculomegaly in Adults (LOVA): Diagnostic Aspects, CSF Dynamics with Lumbar Infusion Test and Treatment Options in a Consecutive Series with Long-Term Follow-Up', *World Neurosurgery*, 156, pp. e30–e40. Available at: https://doi.org/10.1016/j.wneu.2021.08.068.

Varela, M.F., Miyabe, M.M. and Oria, M. (2020) 'Fetal brain damage in congenital hydrocephalus', *Child's Nervous System: ChNS: Official Journal of the International Society for Pediatric Neurosurgery*, 36(8), pp. 1661–1668. Available at: https://doi.org/10.1007/s00381-020-04657-9.

Ved, R., Leach, P. and Patel, C. (2017) 'Surgical treatment of long-standing overt ventriculomegaly in adults (LOVA)', *Acta Neurochirurgica*, 159(1), pp. 71–79. Available at: https://doi.org/10.1007/s00701-016-2998-7.

Virhammar, J. *et al.* (2014) 'Preoperative prognostic value of MRI findings in 108 patients with idiopathic normal pressure hydrocephalus', *AJNR. American journal of neuroradiology*, 35(12), pp. 2311–2318. Available at: https://doi.org/10.3174/ajnr.A4046.

Warf, B.C. (2005) 'Hydrocephalus in Uganda: the predominance of infectious origin and primary management with endoscopic third ventriculostomy', *Journal of Neurosurgery*, 102(1 Suppl), pp. 1–15. Available at: https://doi.org/10.3171/ped.2005.102.1.0001.

'World Medical Association Declaration of Helsinki: Ethical Principles for Medical Research Involving Human Subjects' (2013) *JAMA*, 310(20), p. 2191. Available at: https://doi.org/10.1001/jama.2013.281053.

Xu, H. *et al.* (2022) 'Multiple Machine Learning Approaches for Morphometric Parameters in Prediction of Hydrocephalus', *Brain Sciences*, 12(11), p. 1484. Available at: https://doi.org/10.3390/brainsci12111484.

Yin, R., Wen, J. and Wei, J. (2021) 'Progression in Neuroimaging of Normal Pressure Hydrocephalus', *Frontiers in Neurology*, 12, p. 700269. Available at: https://doi.org/10.3389/fneur.2021.700269.

Appendices

Appendix A

Data management plan

1. Project Name

   A morphometric study of the brain ventricles of patients diagnosed with Chronic Hydrocephalus at Groote Schuur Hospital.

2. Lead principal investigator

   Reagobaka Lichaba

3. Data collection

   Clinical data:

   New quantitative data will be generated from existing patient medical data.
   The UCT Clinical Research Centre has an SOP in place for database construction and security (CRC SOP 08c). The main security risk is the exposure of confidential information. The records will be kept in a secure filing system by the PI and will only be accessible to authorised personnel. Only de-identified data will be stored in the REDCap database, accessible only to authorised study staff with individual passwords and defined user rights. A full-time data manager (or data management team), based at the UCT Clinical Research Centre, will manage the REDCap database including its maintenance, monitoring and access control (including granting of user rights). The Principal Investigator or a delegate will supervise the data management team and oversee the provision of access to the data to authorised individuals. In addition, a professional data manager and data management team supervised by UCT's ICTS department will be responsible for study-wide data management.
   Medical records will be used to collect demographic and clinical data. From these records, data will be entered into the electronic REDCap forms for online storage and management. The electronic REDCap data will be checked for accuracy by authorised study staff, with a dated audit trail for all changes.

Expected dataset types

All the data from the medical records will be entered electronically into REDCap software – a secure web application for building and managing online surveys and databases. All participants will be recruited from a single department – the Radiology Department of Groote Schuur Hospital, in South Africa. The REDCap platform ensures long-term validity and integrity; data can be accessed in a controlled manner and exported in different file formats Microsoft Excel, and IBM SPSS statistics software, among others.

Data Sharing

The intention is to publish the research under CC BY licensing.

Data sharing will be governed by 4 principles:

I. **Protection of participant's confidentiality**

   Confidentiality will be protected according to the **PPI here**.

   Only authorised study staff will have access to the database with defined user rights, and the de-identified data will only be shared on instruction form, and through, the principal investigator in situations deemed reasonable.

II. **Respect for consent agreements**

   Data will only be shared in accordance with detailed and explained agreements in the written consent form, which will be explained in a telephonic discussion.

III. **Protection of intellectual property rights**

   Where appropriate, data sharing will be done with signed agreements to protect intellectual property rights.

IV. **User responsibilities**

All users of study data will be bound by user agreements, including the following:

a. Data may only be shared with users authorised by the Principal Investigator.
b. Study data may only be shared and used for research purposes described in the study proposal.
c. Only de-identified data may be shared. Any identifying information will never be recorded or shared with any other person.
d. Users of study data may not attempt to identify any individual from the provided data unless authorised to do so by the PI for verification.

4. Data storage

Data volumes/storage requirements

Clinical data: the expected size of the data set is minimal.

Data transfer speed

Clinical data: Not applicable.

5. Nominated data centre

Clinical data: ZivaHUB hosted on OpenUCT.

Metadata

Clinical data: Dublin Core Field.

Appendix B

University of Cape Town Human Research Ethics Committee Approval letter

UNIVERSITY OF CAPE TOWN
Faculty of Health Sciences
Human Research Ethics Committee

Room 45 E-52-E-Floor- Old Mair Building
Groote Schuur Hospital
Observatory 7925
Telephone [021] 406 6492
Email: hrec-submissions@uct.ac.za
Website: www.health.uct.ac.za/home/human-research-ethics

27 February 2023

HREC REF: 700/2022

Dr K Mpolokeng
Division of Clinical Anatomy & Biological Anthropology
FHS
Email: Kentse.mpolokeng@uct.ac.za
Student: lchrea001@myuct.ac.za

Dear Dr Mpolokeng

PROJECT TITLE: A MORPHOMETRIC STUDY OF THE BRAIN VENTRICLES OF PATIENTS DIAGNOSED WITH CHRONIC HYDROCEPHALUS AT GROOTE SCHUUR HOSPITAL (MASTER'S DEGREE - MISS REAGOBAKA LICHABA)

Thank you for your response letter, addressing the issues raised by the Faculty of Health Sciences Human Research Ethics Committee (HREC).

It is a pleasure to inform you that the HREC has **formally approved** the above-mentioned study.

Approval is granted for one year until the 28 February 2024.

Please submit a progress form, using the standardised Annual Report Form (FHS016) if the study continues beyond the approval period. Please submit a Standard Closure form if the study is completed within the approval period.
(Forms can be found on our website: www.health.uct.ac.za/fhs/research/humanethics/forms)

The HREC acknowledge that the student: Miss Reagobake Lichaba will also be involved in this study.

Please quote the HREC REF 700/2022 in all your correspondence.

Please note that the ongoing ethical conduct of the study remains the responsibility of the principal investigator.

Please note that for all studies approved by the HREC, the principal investigator **must** obtain appropriate institutional approval, where necessary, before the research may occur.

Yours sincerely

Signed by candidate

PROFESSOR M BLOCKMAN
CHAIRPERSON, FACULTY OF HEALTH SCIENCES HUMAN RESEARCH ETHICS COMMITTEE

Appendix C

Groote Schuur Hospital Approval letter

Western Cape Government

GROOTE SCHUUR HOSPITAL

Enquiries: Dr Bernadette Eick
E-mail: GSHResearch.Request@westerncape.gov.za

Dr Kentse Mpolokeng
Division of Clinical Anatomy and Biological Anthropology

Email: kentse.mpolokeng@uct.ac.za

Dear Dr K Mpolokeng,

RESEARCH PROJECT: A MORPHOMETRIC STUDY OF THE BRAIN VENTRICLES OF PATIENTS DIAGNOSED WITH CHRONIC HYDROCEPHALUS AT GROOTE SCHUUR HOSPITAL.

Your recent letter to the hospital refers.

You are granted permission to proceed with your research, which is valid until **28 February 2024.**

Please note the following:

a) Your research may not interfere with normal patient care.
b) Hospital staff may not be asked to assist with the research.
c) No additional costs to the hospital should be incurred as indicated in your Annexure 2 i.e. Lab, consumables or stationery. **If access to TRACK Care/NHLS is required, kindly attach our letter of approval to the application form and approach Information Management to assist with data.**
d) **No patient folders may be removed from the premises or be inaccessible.**
e) Please provide the research assistant/field worker with a copy of this letter as verification of approval.
f) Confidentiality must always be maintained.
g) Once the research is complete, please submit a copy of the publication or report.
h) **Please adhere to ALL COVID-19 regulations and Groote Schuur Hospital policies.**
i) **All Clinical Trials to be registered on Clinicom with Michelle Riley or Rowan James,** michelle.riley@westerncape.gov.za / rowan.james@westerncape.gov.za

G46 Management Suite, Old Main Building,
Observatory 7925

Private Bag X,
Observatory, 7935

Tel: +27 21 404 6288 fax: +27 21 404 6125
www.westerncape.gov.za/health

I would like to wish you every success with the project.

Yours sincerely

Signed by candidate

DR BERNADETTE EICK
CHIEF OPERATIONAL OFFICER
Date: 12 May 2023

C.C. Prof Ntusi, Dr Khumalo, A/Prof Fieggan and Mr. A. Mohamed

Appendix D

Groote Schuur Hospital - Radiology Department Approval letter

GROOTE SCHUUR HOSPITAL **UNIVERSITY OF CAPE TOWN**

RADIOLOGY DEPARTMENT
Groote Schuur Hospital, Private Bag, Observatory 7935, South Africa
Telephone (021) 404-4184. Residence (021) 794-4054
Fax No. (021) 404-4185
Internet Address Sulaiman.moosa@uct.ac.za
Head of Division: **Assoc. Prof. Sulaiman Moosa**
April 3. 2023

To whom it may concern,

This letter is to confirm that Reagobaka Lichaba has approval from the Department of Radiology to use images from the department in her study looking at A Morphometric Study of the Brain Ventricles of Patients Diagnosed with Chronic Hydrocephalus at Groote Schuur Hospital.

Sincerely,

Signed by candidate

Assoc. Prof. S Moosa
Head: Division of Radiology

Appendix E

Data collection sheet

Study number	Age (Years)	Sex (Female, Male)	Presenting history	Clinical findings	Relevant findings	Diagnosis from doctors assessment (Positive/ Negative)	Was the patient treated? (Yes/No)	Type of operation	Evans Index	Evans Index ave.	Temporal Horns Width (mm)				Intracranial pressure measurement	Frontal Horns
									Ratio (R) = (Frontal horn width (FH)/ Max inner cranial plate)		Left	Left ave.	Right	Right ave.		Quadrilateral or Round (Oval)

Third ventricle			Sylvian Fissures								Callosal Angle (^{o})	Callosal Angle ave.	Periventricular white matter changes						
			Length (mm)				Width (mm)							Left (√/X)			Right (√/X)		
Width (mm)	Width ave.	Shape	Left	Left ave.	Right	Right ave.	Left	Left ave.	Right	Right ave.			PWMC	Present around frontal horns	Present around temporal horns	Spread around lateral ventricles body	Present around frontal horns	Present around temporal horns	Spread around lateral ventricles body